Implementation and Evaluation of Fluid-Structure-Interaction for Propellers

Auteur : Madathy Parambil Asif, Adhil
Promoteur(s) : 14928
Faculté : Faculté des Sciences appliquées
Diplôme : Master : ingénieur civil mécanicien, à finalité spécialisée en "Advanced Ship Design"
Année académique : 2020-2021
URI/URL : http://hdl.handle.net/2268.2/13507









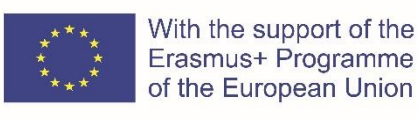


Implementation and evaluation of Fluid- Structure interaction for propeller

Submitted on 25 August 2021

By,

Madathy Parambil Asif Adhil

Student ID No.:200541E

First Reviewer:

Dr.Alban Leroyer

École Centrale de Nantes

Nantes,France

Second Reviewer:

Dr.Antoine Ducoin

École Centrale de Nantes

Nantes, France

This page is intentionally left blank

ABSTRACT

The thesis aims to implement and evaluate a one-way Fluid-structure coupling for propellers. In this context, the focus is to study the influence of scaling effects as most hydrodynamic evaluations of propeller performances are carried out at model scale and structural analysis at full scale. To understand the differences, all calculations are performed in both scales. Hydrodynamic influences are compared between the scales and structural analysis analyses are compared between scaled model scale vs. full scale. The thesis, also aims to propose a reduced method of evaluating hydrodynamic performances, as this part of the evaluation is the most time consuming.. The reduced evaluation shows promising results and faster convergence with lower computational cost.

Table of Contents

List of Figures

List of Tables

Declaration of Authorship

I declare that this thesis and the work presented in it are my own and have been generated by me as the result of my own original research.

Where I have consulted the published work of others, this is always clearly attributed.

Where I have quoted from the work of others, the source is always given. With the exception of such quotations, this thesis is entirely my own work.

I have acknowledged all main sources of help.

Where the thesis is based on work done by myself jointly with others, I have made clear exactly what is done by others and what I have contributed myself.

This thesis contains no material that has been submitted previously, in whole or in part, for the award of any other academic degree or diploma.

I cede copyright of the thesis in favour of the University of Ecole Centrale Nantes

Date: 25/08/2021 Signature:

This page is intentionally left blank

1. **INTRODUCTION**

Ships have been around for centuries and have been an integral part of the transportation network. Shipping contributes to around 90% of the movement of world's commodities. Therefore efficiency and reliability are the cornerstones of this industry. Much complex engineering and design goes into building a ship. One of the most complex and important engineering and design work is done in powering the vessels. A good power train is required for optimum performance and to ensure adequate speed is achieved. Most ships are powered by massive two-stroke diesel engines. This engine is connected by a shaft to a rotating device which converts the rotational force to translational force. This device is called a propeller (Figure 1.1).

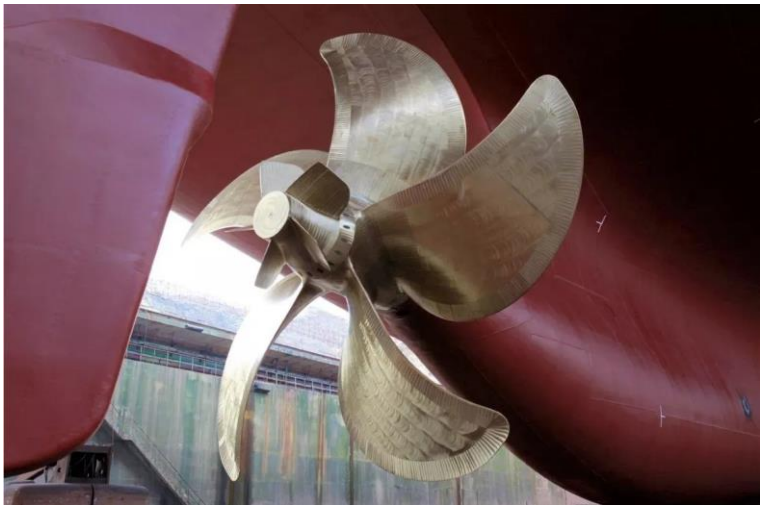

Figure 1. 1 : Ship propeller (MMG)

A propeller consists of blades having an aerofoil section which when rotated in fluid medium produces lift. This lift force (often called as thrust) provides enough push to move the ship forward at desired speed. A badly designed propeller will not be able to propel the ship to the required speed and will also lead to higher fuel consumption. A bad design could also lead to hull vibration and noises. Therefore, hydrodynamic analysis of propellers is important to produce an efficient power train.

Of course, a highly efficient propeller is of no use if the propeller cannot withstand the forces acting on it. The strength analysis of propellers is therefore necessary to ensure safe operation of the vessel and the safety of the crew. It is critical that the designed propeller is able to withstand loads acting on it as loss of propulsion could lead to unmovable ship or loss of control of the vessel. It also has to be designed for impact as well because a ship without propulsion is dangerous to the crew onboard and vessels or structures nearby.

The cost of the propeller depends highly on the weight of the propeller. Most structral aspects of the propellers are defined by the classification society. The classification society defines the thickness of the propeller blades. These defined thicknesses are usually more than what is required for safe operation of propellers. The traditional method of scaling the results by ITTC 1978 scaling method uses a Reynolds number based frictional correction for model test results to full scale extrapolation (ITTC , 2008).This has been followed by most model test facilities and mostly used by classification societies for structural specifications. This method is shown to have major failings when it comes to high skew propellers, large area coefficient and also for tip modified propellers (Shin .et al, 2017). This leads to overdesigned propellers with unnecessary proportions and ultimately cost.Therefore, there is a need to evaluate the exact loads acting on the blade of the propeller to reduce the weight and cost associated with propeller design and construction.

By performing fluid structure interaction the extact loads acting on the propeller can be extracted for structural analysis.This thesis aims to develop a coupled analysis to evaluate both the hydrodynamic load and the resulting structural loads and deformation occurring on the propeller. The loads extracted from hydrodynamic analysis is coupled with structural analysis by using pressure forces acting on the blade to estimate the stresses and deformation associated with the propeller.

2. THEORY

A propeller is a device which when rotated in fluid medium produces lift. The lift is generated because each leaf of the propeller (called blades) has an aerofoil section. When the aerofoil section encounters incoming flow, the foil generates lift. Like, any aerofoil section, the propeller also has a leading edge and a trailing edge. The edge which encounters the flow first is called the leading edge and the edge where the flow exits the section is called a trailing edge. The blades of the propeller are connected to a hub/boss which is connected to a shaft which rotates. The edge of the blade which attaches to the hub is called as root of the blade and the farthest point of the blade is called as tip of the blade. The diameter (D) of the propeller is twice the distance from one tip to propeller axis. The portion of the blade where high pressures are generated is called pressure side or face. The portion of the blade where low pressures are created are called suction side or back. Figure 2.1 shows the basic terminology of propellers.

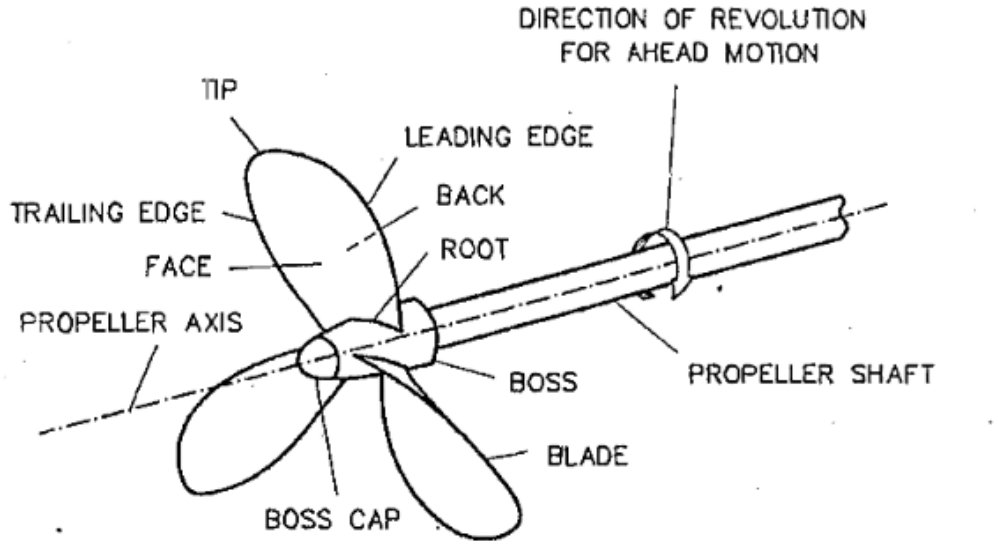

Figure 2. 1: Propeller geometry and terminology (Ghose and Ghokarn, 2004)

Propellers of these sorts are called screw propellers. This is because propeller blades when rotated, each section follows a helical path, just like threads on a screw. The longitudinal distance travelled by a propeller per revolution is called as pitch (P) of the propeller. The lift generated by each section of the blade depends on the inflow (V_A, m/s) onto the blade and the rotation rate (n) of the propeller. This leads to an angle of attack which creates lift (Figure 2.2).

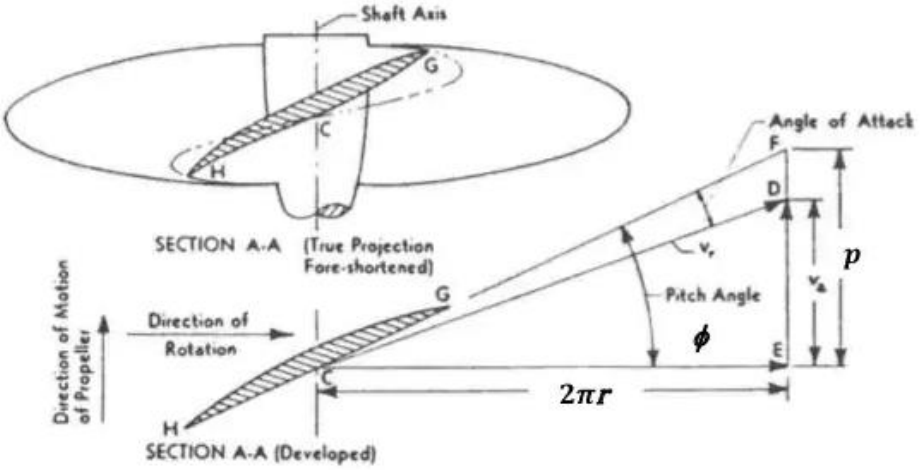

Figure 2. 2 : aerofoil section and lift generation mechanism(http://web.mit.edu/2.016/www/handouts/2005Reading10.pdf)

2.1 Model testing

Ship power prediction begins with the estimation of resistance of ship. Ship resistance is predicted by towing tank test, where a scaled down model is towed at desired speed, V_s (m/s) to estimate the resistance, R_{TM} (Newton) experienced by the hull. Once the resistance is predicted, the power required to propel the ship is determined (Effective power, P_E (Kw)) (equation 1).

$$P_E = R_{TM} V_s \quad (1)$$

The propeller is to be designed at this power; although a small modification of this power is explained in Section 2.1.2 .The designed propeller needs to be tested to predict its performance. The performance of the propeller is tested in scaled down geometry of propeller. Scaling down propeller requires the laws of similarities to be maintained. Namely; geometric similarity, kinematic similarity and dynamic similarity. The geometric similarity requires that the model be geometrically similar to the full-size body. This is achieved by direct scaling down of prototype using scale ratio (λ). Kinematic similarity is maintained to ensure that for each geometrically similar faces the resultant direction of velocity component are identical. For propellers , this is achieved by considering inflow velocity or velocity of advance (V_A) and circumferential speed (equation 2).

Advance coefficient, $J = \frac{V_A}{n\,D}$ (2)

Where,

V_A (m/s) is velocity of advance (inflow velocity)

n is rotation per second

Dynamic similarity requires ratios of forces such as Inertia forces, gravity forces, viscous forces and pressure forces to remain identical. But in practice, Froude similarity (Inertia forces/Gravity forces) is only maintained for most calculations. Maintaining both Froude similarity and Reynolds similarity (Inertia forces/Viscous forces) would require the model scale to be similar in size to prototype scale. Therefore, Reynolds similarity is not maintained, but in most test conditions the RPS of the propeller is given a high value to reduce the effect of neglecting Reynolds similarity. Euler similarity (Pressure forces/Inertia forces) is automatically maintained because of the geometric similarity of the propeller and since, hydrostatic pressure is proportional to the depth of immersion and hence to the propeller diameter, provided caviation does not occur (Ghose and Ghokarn, 2004).

2.1.1 Open water test

Open water condition is performed to study the characteristics of the propeller in open stream i.e. without the influence of hull. The test is performed in a flume facility or towing tank which can produce a constant flow velocity in controlled environment. The inflow velocity and depth of the test are controlled by the flume or towing carriage speed and rotation speed of the propeller is changed using a motor and the force acting on the propeller is monitored and recorded during the experiment.

The open water test device is used to control propeller rotation speed, provide fixed support and measure forces (Figure 2.3).The device consists of a propeller, hydrodynamic balance and a motor. The propeller rotation is controlled by the motor and an electrical control setup. The thrust and torque forces acting on the propeller are measured by the hydrodynamic balance which is a dynamometer.

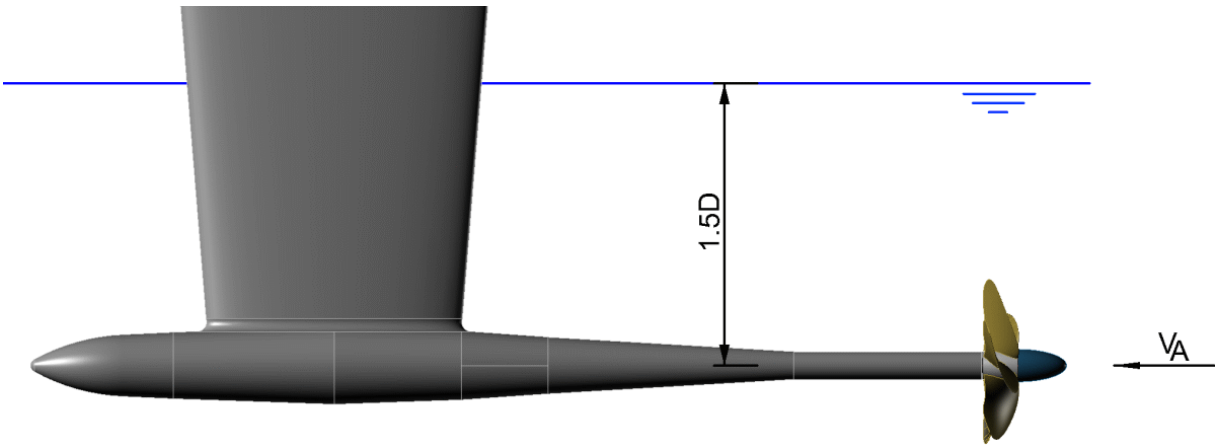

Figure 2. 3: Open water test device (https://www.sva-potsdam.de/en/open-water-test/)

Propeller characteristics are determined using the following non dimensional values (Ghose and Ghokarn, 2004).

The thrust and torque are non-dimensionalised as follows,

Thrust Coefficient, $K_T = \frac{T}{\rho\, n^2 D^4}$ (3) Where,

T is thrust (N)

ρ is density (Kg/m^3)

Torque Coefficient, $K_Q = \frac{Q}{\rho\, n^2 D^5}$ (4) Where,

Q is torque (N.m)

Open water efficiency, $\eta_o = \frac{TV_A}{2\pi nQ} = \frac{K_T\, J}{K_Q\, 2\pi}$ (5)

The efficiency defines the ratio between power (TV) produced by the propeller and power given by the motor ($2\pi nQ$).

2.1.2 Self Propulsion test (Behind ship condition)

Although open water test is an important part of designing the propeller and evaluating the propeller characteristics, the test is performed in open stream condition. But propellers are designed to operate behind a ship's hull. The determination of propeller characteristics operating behind a ship's hull is known as behind ship condition. In this condition, the propeller does not experience a uniform flow similar to that of an open water test, instead experiences ship wake as inflow. Wake is the disturbed flow behind an object travelling in

fluid. The wake depends on the shape of the body and the speed it is travelling at for a particular fluid medium. For propeller performance analysis, all wakes are defined at the propeller plane aft of the ship. Two types of wake are typically recognised while analysing propeller characteristics; nominal wake and effective wake. Nominal wake is the measured values of velocities at the propeller plane when ship is moving at a particular speed (V_s) without the propeller i.e. during resistance test. Effective wake is the measured values of velocities at the propeller plane when ship is moving at a particular speed (V_s) with the propeller under operation i.e. during propulsion test. The effective wake will be faster than nominal wake due to propeller suction. These velocities are usually demonstrated as wake profiles. Difference in wake profiles between nominal wake profile and effective wake are shown in Figure 2.4.

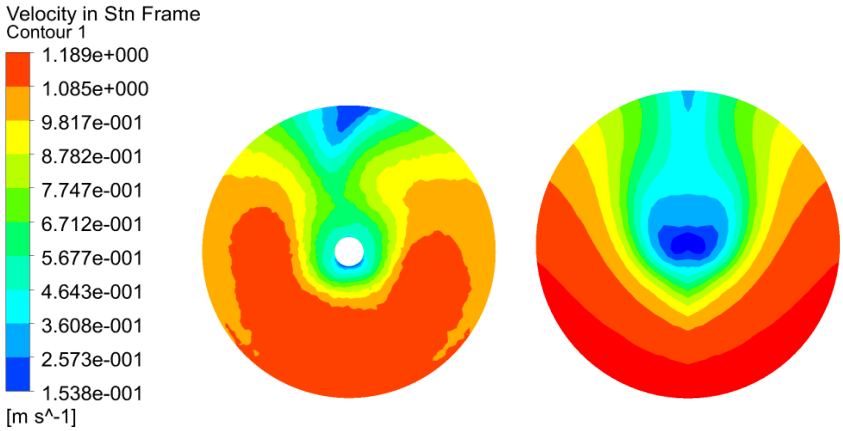

Figure 2. 4: Effective wake (left) and Nominal wake (right)

Figure 2.4 shows the wakes of ship defined in section 3.1 at velocity of 1.315 m/s in model scale. The noticeable differences in wake profiles are of importance for propeller analysis. The inflow onto the propeller varies according to the wake. This affects the propeller performance in behind ship condition. An important term to be understood while calculating performance is velocity of advance (V_A). Velocity of advance is the inflow velocity experienced by the propeller at the propeller plane. In open water condition, the inflow is uniform and therefore this can be taken as the velocity of advance (V_A). But, due to the presence of wake, the inflow experienced by the propeller blades are different at each degree of rotation and therefore the thrust developed is also different. To non-dimensionalise the influence, a concept of wake fraction is used and is defined by,

$$\text{Wake fraction, } w = \frac{V_S - V_A}{V_S} \quad (6)$$

Where, V_A is taken as an average value of the wake profile. The wake fraction is considered as constant and therefore at any ship velocity, V_A can be found. This would result in an average wake fraction across the propeller plane.

In order to assess the performance of the propeller behind the ship, a self-propulsion test is carried out. The self-propulsion test is carried out in a towing tank facility. The ship at model scale is fitted with the propeller and is towed at desired speed using a tow rope. The tow rope is attached to a dynamometer. It is to be noted that the test is performed under Froude similarity. In model scale the Reynolds similarity is not maintained and therefore the resulting frictional drag component of ship will be higher because frictional drag reduces with increase in Reynolds number. To compensate an extra force is applied as a small weight (F_D) (Bertram ,2012). The entire experimental setup is shown in Figure 2.5.

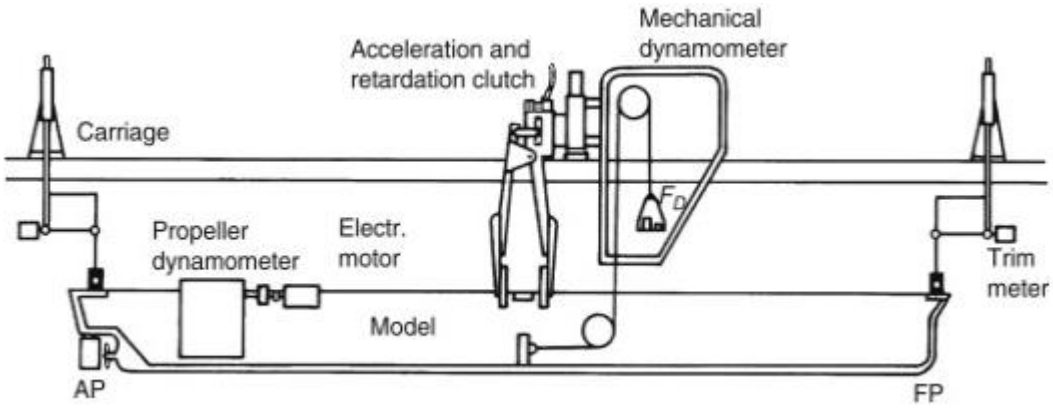

Figure 2. 5: self-propulsion setup (Bertram,2012)

The ship hull experiences an increase in resistance due to the action of propeller behind the ship. The propellers sucks the flow and reduced the pressure on the aft of the ships hull. This is quatified as thrust deduction fraction, *t* and therefore R_{TM} in equation 1 becomes

$$t = \frac{T + F_D - R_{TM}}{T} \tag{7}$$

Where, T is thrust from propeller.The propeller is fitted to a dynamometer to measure thrust and torque and an electric motor for drive. The propeller rpm is increased incrementally until the ship is completely propelled by the thrust (T_P) produced by the propeller i.e. when the dynamometer value becomes zero. The thrust (T_P) and torque (Q_P) produced by the propeller are noted from propeller dynamometer.

Using these results the concept of thrust identity is applied. The evaluated K_T and K_Q from the self-propulsion test are compared with open water test propeller curves and the J value is then determined from open water curves.

2.1.3 Full scale performance

The model scale results are run at high RPS and the diameter is very small compared to full scale. This causes flow changes around the propeller. Mainly, the changes are viscous in nature as the full scale propellers predominantly have turbulent flow on blade surfaces it is not necessarily the case in model case. Model scale results suffer from laminar flow effects. It is to be noted that higher RPS in model scale produces better results as Reynolds number increases. But there exists a change in propeller characteristics. While the thrust remains unaffected, the torque changes as viscous nature changes at the blade surface. Although there are many methods to predict these changes, the most commonly used is 1978 ITTC performance prediction method. This method provides a correction of K_T and K_Q based on propeller section characteristics and local Reynolds number at 0.7 Radius (R) (John Carlton, 2007).

2.2 Strength calculation of propellers

The strength of the propeller determines its ability to withstand loads. Usually, the thickness of the blade is defined by classification rules based on the number of blades, power, rate of revolution (RPS) and other parameters. Rules of one such classification society can be seen in Germanischer Lloyd (2017).But it is often found out that the propeller blades do not require such high thickness. The inconsistency in the rule based thickness between different classification societies also makes these values questionable. With advancement in computer performances Finite Element Analysis (FEA) has shed some light in this area. It is often found that the thickness provided by the classification societies usually over predicts the thickness. Propeller manufactures have therefore resorted to propeller strength calculation using FEA analysis to reduce the thickness, which saves material and ultimately cost. These methods of predictions have been accepted by the classification society.

The propeller is designed at maximum torque point of the engine. This is usually above the operational point and assumes worst case of propeller loading. Stress values are assessed in terms of Von-Mises stresses as well as Principal stresses. These stress values are often

compared with the maximum allowable stresses the classification society prescribes. Given that the values given by classification societies are way below the strength of the material usually means that the propellers are in any case over designed. This is crucial as propulsion should always be maintained to ensure the safety of the crew and ship itself.

2.3 Computational fluid dynamics (CFD)

CFD is a branch of fluid mechanics which uses numerical analysis and data structure to solve complex fluid flow. The governing equation is Navier-Stokes (N-S) equation. But this equation can be simplified to Euler's equation by neglecting viscous terms and further to potential equations by removing vorticity. A CAD domain describes the boundaries and volume, this is called as domain. The domain is discretized into smaller regions connected to each other forming a grid. The grid could be structured (has order) or unstructured. Boundary conditions are applied to boundary surfaces. The governing equation is then solved continuously at incremental increase in time to simulate the flow.

In the context of this thesis, the governing equation is Reynolds Averaged Navier-Stokes equation (RANSE) which is used to solve turbulence modelling at reduced computational cost. To solve the turbulence modelling the equation introduces new terms called Reynolds stresses which are apparent stresses. The introduction of these terms causes the equation to be open and to close this equation the Reynolds stresses can be determined algebraically with turbulence models. This could be one equation model, two equation model or empirical formula giving various levels of sophistication and application (Mert Gokdepe, 2015). Commercially available RANSE based CFD software known as ANSYS CFX is used for all simulation in this thesis.

2.4 Finite element Analysis (FEA)

Finite element analysis is used to solve partial differential equation numerically. It subdivides the domain into discrete elements known as finite elements which are then connected together to form mesh This numerical domain now consists of a finite number of points which can now be formulated as a boundary value problem. This can be represented as a system of equation which can then be solved by assembling it into a matrix format. The solution

provides an approximate value at each finite point of the domain and then interpolation between the points gives solutions at each point of the domain.

In the context of this thesis, FEA is used to determine the structural deformation and stresses. The mesh used is unstructured and the governing equation is

$$F = K\,U \tag{8}$$

Where F is the force applied, K is the stiffness of the material and U is the displacement associated with it. The problem is defined by applying the load, stiffness by defining the material and applied boundary conditions. The solution to this problem becomes displacement at each finite point. The stress, strain and all other structural characteristics can then be derived from relations based its relation with the displacement (deformation). The FEA software used for structural analysis is commercial software called ANSYS Mechnaical.

3 TEST CASE

3.1 Propeller geometry

The propeller used throughout this report is a MMG developed propeller .The CAD geometry of propeller is shown below in Figure 3.1.

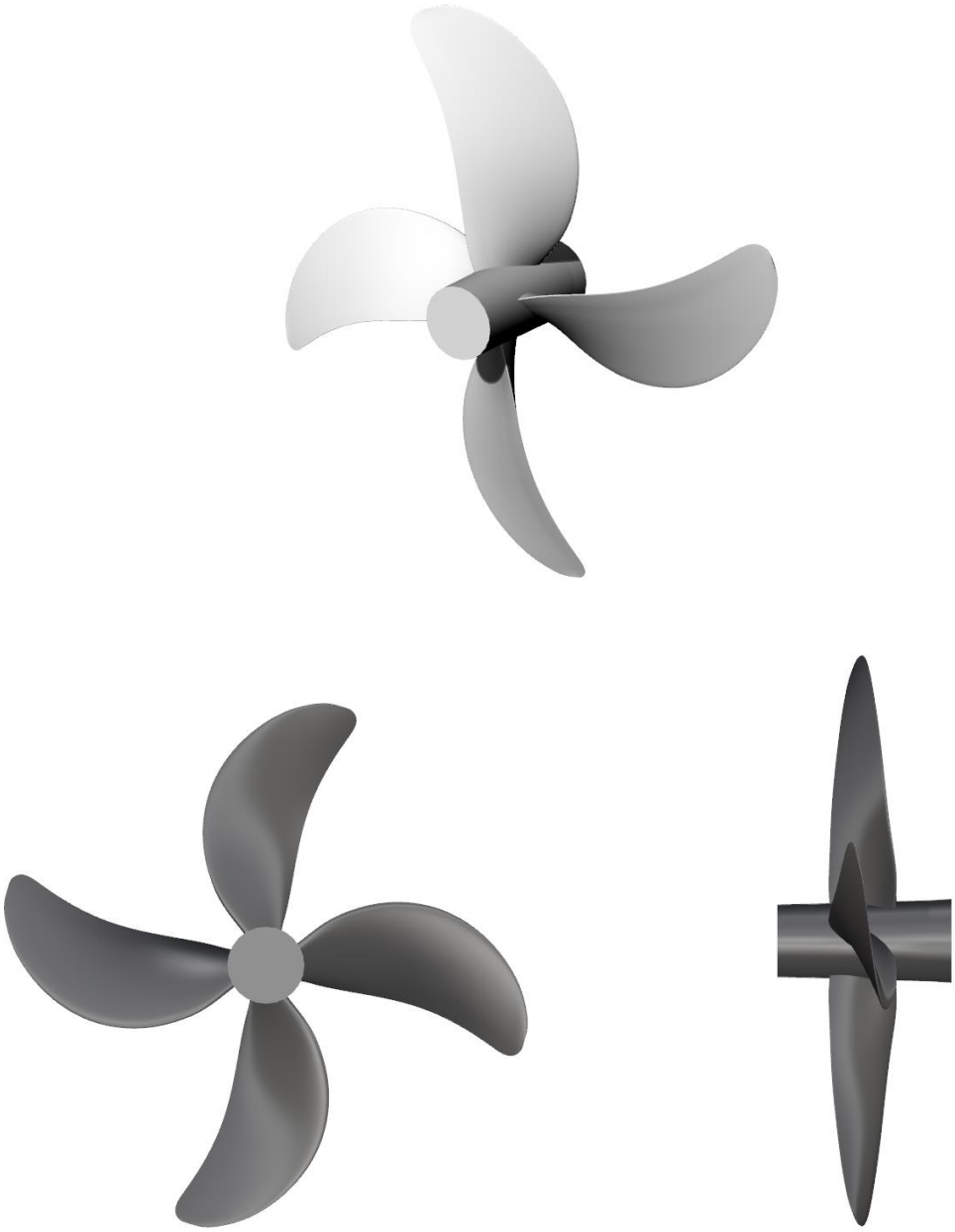

Figure 3. 1 : Propeller geometry in perspective view (top) , front view (left) and side view (right)

The Full scale data of the propeller is shown in Table 3.1.The propeller is scaled down with scale ratio of 1/30 to perform all calculation in model scale .

Characteristics	Value	Units	Comment
Diameter (D)	6.3	m	-
Number of blades (Z)	4	-	-
Pitch (P) / Diameter(D)	0.76153	-	at 0.75 D
Chord	1.3119	m	at 0.75 D
Direction of rotation	Right	-	-
Expanded blade area ratio (A_E/A_o)	0.4	-	-
Scale ratio (λ)	1:30		

Table 3. 1: Full scale data of propeller

3.2 Ship geometry

The propeller is designed for a bulk carrier. The ship CAD geometry is shown in Figure 3.2

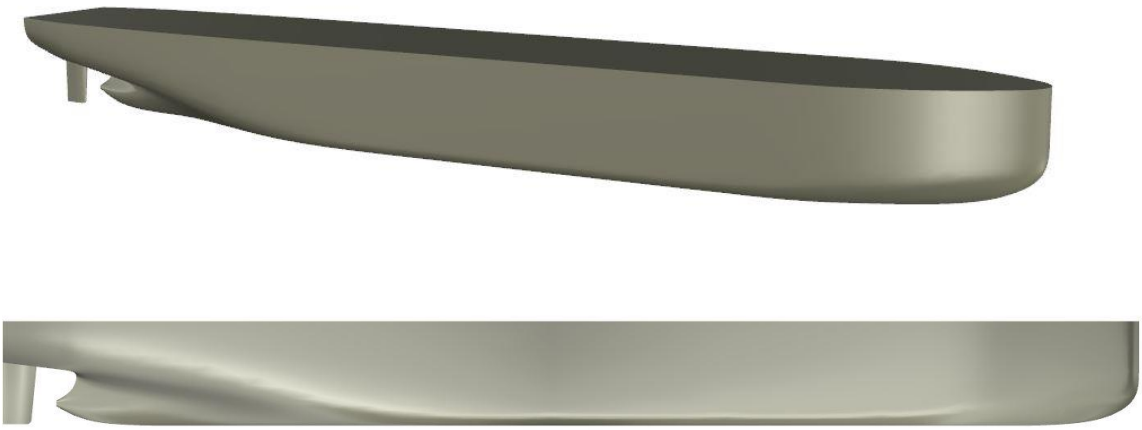

Figure 3. 2: Ship geometry in perspective (top) and profile (bottom) views

The full scale data of ship and the models scale data of ship are shown in Table 3.2.

Characteristics	Value		Units
	Model scale	Full scale	
Length between perpendicular (L_{pp})	6	180	m
Length of waterline (L_{WL})	6.15	184.5	m
Beam (B)	1	30	m
Draft (T)	0.35	10.5	m
Block Coefficient (CB)	0.7941	0.7941	-
Scale ratio (λ)	1:30		

Table 3. 2: Full scale and model scale data of ship

3.3 Operational condition

Open water tests are performed in model scale and operational condition for open water (OCO) is mentioned below in Table 3.3.

Operational condition	J	Inlet Velocity (m/s)
OCO 1	0.45	1.701
OCO 2	0.5	1.89
OCO 3	0.55	2.079
OCO 4	0.6	2.268
OCO 5	0.65	2.457
OCO 6	0.8	3.024
propeller RPS (1/s)	18	

Table 3. 3: Operational conditions for open water

For behind ship simulations, the conditions performed in section 6 are direct comparison to self-propulsion test performed (OCB 1) in towing tank and a full scale simulation performed by scaling. The operational conditions for behind ship (OCB) are shown in Table 3.4.

Characteristics	Model scale	Full scale
	OCB 1	OCB 2
J	0.4458	0.4458
Vs (m/s)	1.315	7.202
RPS (1/s)	7.953	1.452

Table 3. 4: Operational condition for behind ship

3.4 Sign convention

The zero positions of the coordinate system are always placed at intersection between the propeller shaft axis and propeller plane. The sign conventions used in the entire report are as follows

1. Positive X axis is oriented towards downstream of propeller.
2. Positive Y axis is oriented towards starboard side of ship
3. Positive Z axis is oriented upwards towards to deck

All positive errors mentioned in this thesis when comparing to experimental results indicate over prediction of simulation results. All positive errors indicated when comparison is made between full scale simulation and model scale simulation indicates over prediction of model scale values.

4 NUMERICAL ESTIMATION OF OPEN WATER TEST

To test the open water condition a steady numerical RANSE solver of commercial CFD package ANSYS CFX is used. A k-ω SST turbulence model is used and propeller is run at high RPS to eliminate the possibility of laminar effects. A steady state simulation with incompressible flow is used to simulate this condition. The propeller is studied at model scale to asess the mesh and propeller charcteristics. Operational condition from OCO 1 to OCO 6 are simulated in this section.

4.1 Numerical setup

A domain known as “piece of cake” is used to simulate the open water characteristics. The domain is a quarter cylinder with two domains; inner and outer domain (Figure 4.1).

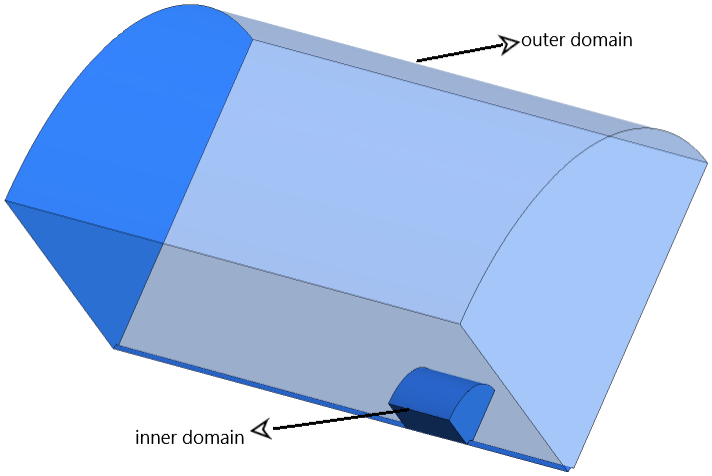

Figure 4. 1: Inner and outer domains

The dimensions of the domain are shown below in Figure 4.2 and Figure 4.3.

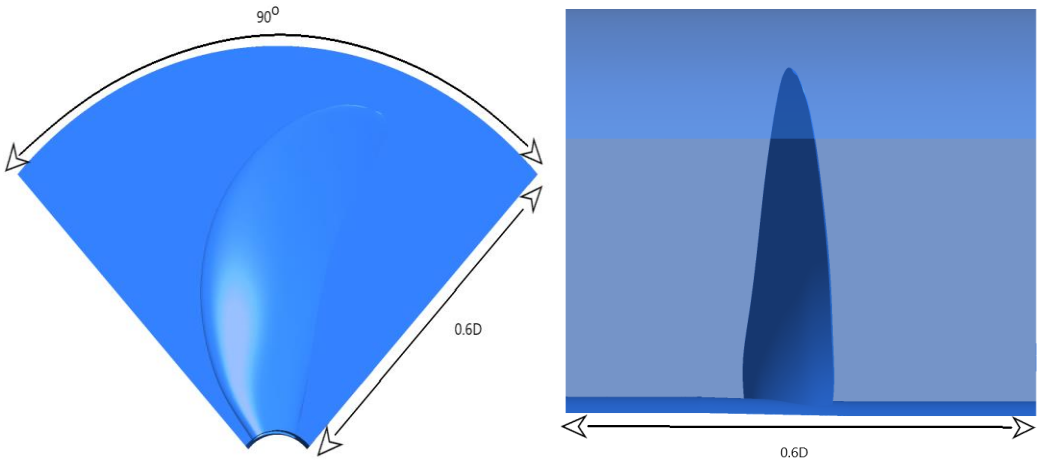

Figure 4. 2: Inner domain dimensions

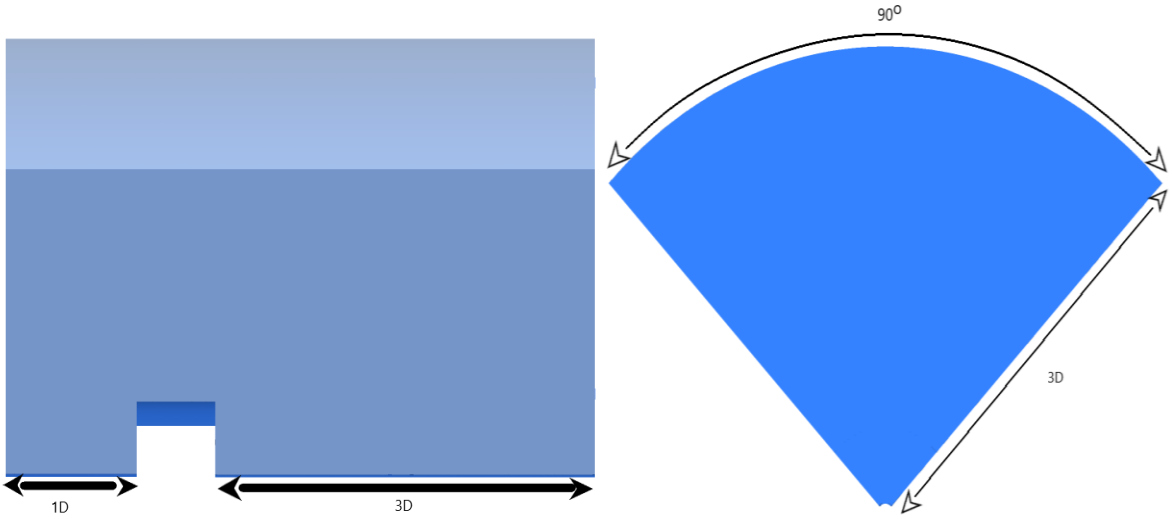

Figure 4. 3: Outer domain

The inner domain is a small quarter cylinder and consists of a single blade with hub. It is a rotating domain with period boundary conditions applied at two ends to emulate nearby blades. An interface condition is used to interpolate values between outer and inner domain. The boundaries used for inner domain is shown in Figure 4.4.

The outer domain is a large stationary quarter cylinder. This domain is used to provide constant velocity to the inner domain (Figure 4.5). The combination of inner and outer domain creates a numerical model of open water test. The analysis is performed for single phase setup with water as fluid medium with density of 997 kg/m^3 corresponding to water temperature of 25 ^oC.

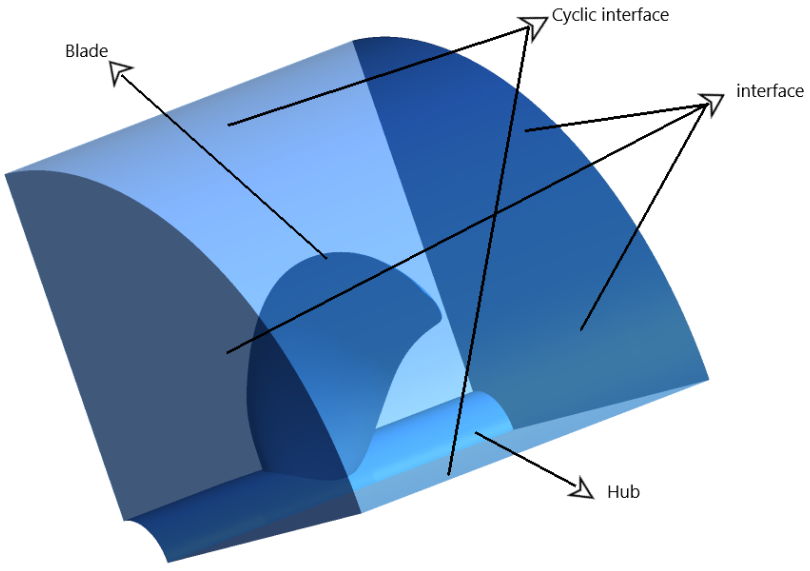

Figure 4. 4: Inner domain boundary condition

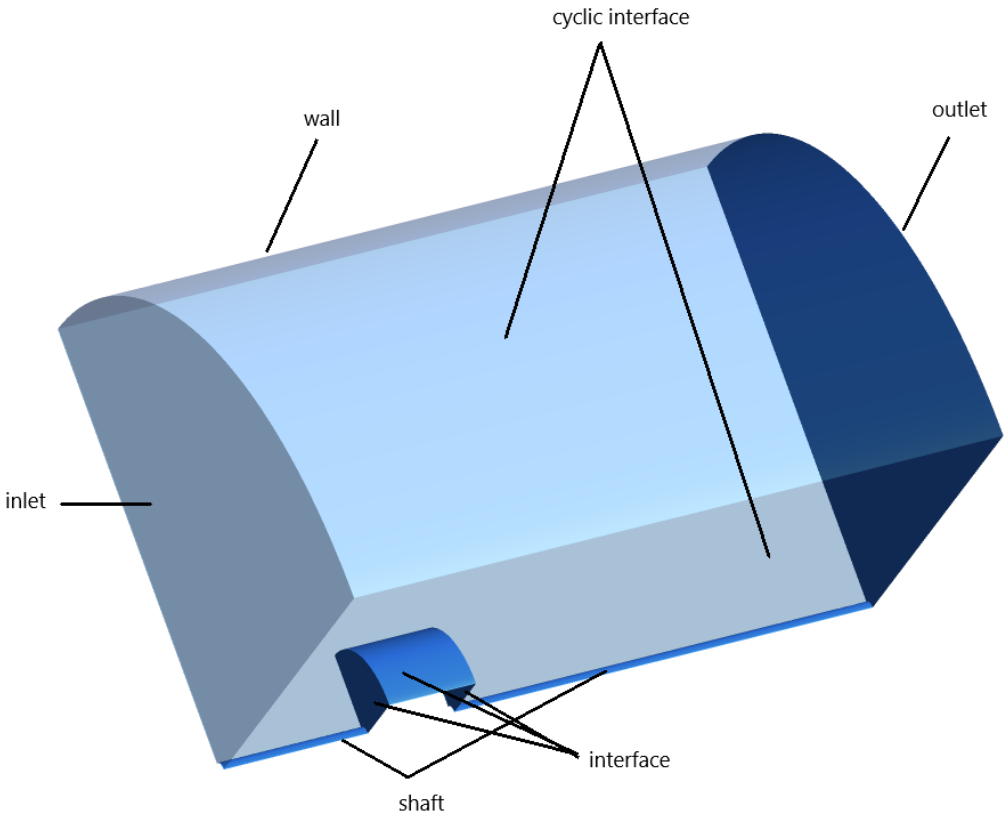

Figure 4. 5: Outer domain boundary condition

The boundary conditions applied to inner domain and outer domain are shown in Table 4.1 and Table 4.2 respectively.

Boundary	**condition**
Interface	frozen interface
Cyclic interface	cyclic condition
Blade and hub	No slip wall

Table 4. 1: Inner domain Boundary conditions

Boundary	**condition**
Inlet	velocity inlet
Cyclic interface	cyclic condition
side wall and shaft	Free slip wall
Outlet	pressure outlet
interface	interface condition

Table 4. 2: Outer domain Boundary conditions

4.2 Mesh and Mesh dependency

The inner and outer domains are meshed separately. The outer domain is meshed without inflation layer and inner domain is meshed with more refinement with the addition of inflation layers to capture boundary layer. Tetrahedral mesh is used to mesh both the domains. Figure 4.6 to Figure 4.7 shows meshes in inner and outer domain

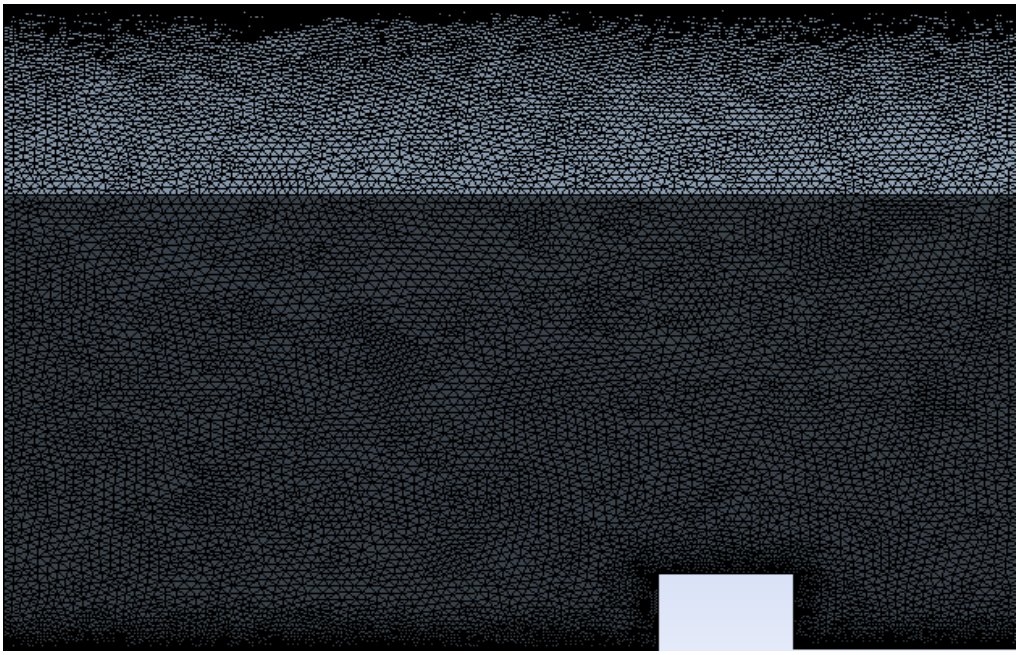

Figure 4. 6: Outer domain Mesh

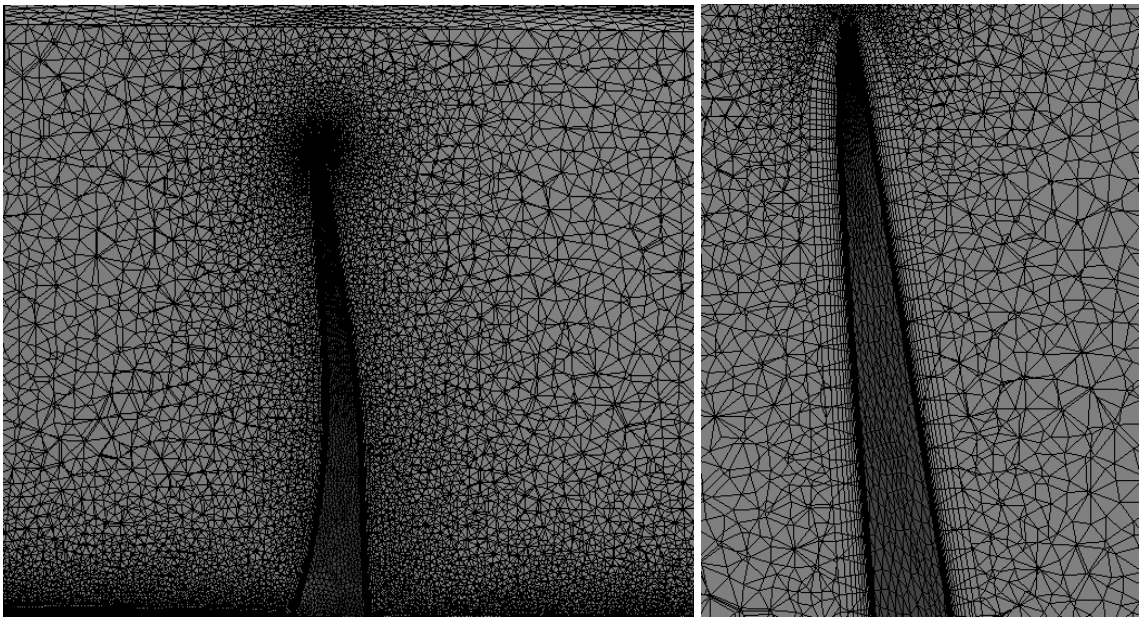

Figure 4. 7: Inner domain Mesh

A surface refinement is applied to blade and hub of the inner domain to ensure proper capture of leading and trailing edges and for proper capture of forces acting on it. The inner domain is also meshed significantly finer compared to outer domain. . The first layer thicknesses of the mesh at No-slip walls are given a value suitable to ensure that the wall Y+ is less than 1. A smooth transition between the final inflation layer and the outside cells is ensured by changing number of layers of inflation and growth rate of the inflation layer.A grid dependency study is performed to ensure that the results are independent of the mesh used. In order to study the grid dependency; thrust produced by the blades at different J is used as variable. The inner domain is refined to study the change in thrust obtained while keeping the inflation layer the same. Figure 4.8 shows the results of grid dependency study.

The dependency study shows that the change in thrust from 5.2 million cells to 7.2 million cells is 0.7 % at J=0.45 and at J=0.8 the change is 1.4 % .Since, change is minimal, the mesh setup of 5.2 million cells is considered for further analysis of open water simulation to save computation time and cost.

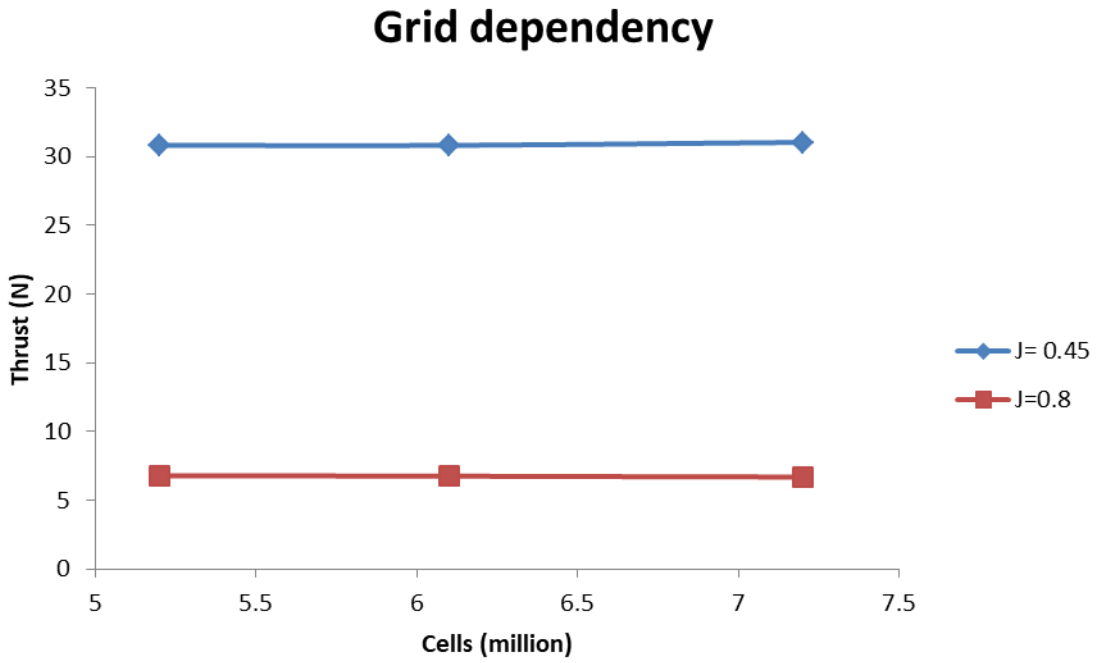

Figure 4. 8: grid dependency

4.3 Results and discussion

The inlet velocities are varied according to the corresponding J value with RPS (n) of the propeller kept constant throughout the simulation. The simulation starts at J value of 0.45 and the result files of this simulation is used as the initial condition for the following simulation at J value of 0.50 and so on. This is done to decrease computation time and provide better initial

condition for subsequent simulations. Figure 4.11 shows the velocity of water in x-direction at section plane cut at the centre of the domain. The suction caused by the propeller upstream of the blade and the increase in velocity downstream of the blade can be clearly seen. Figure 4.9 and Figure 4.10 shows convergence through residual and force respectively.

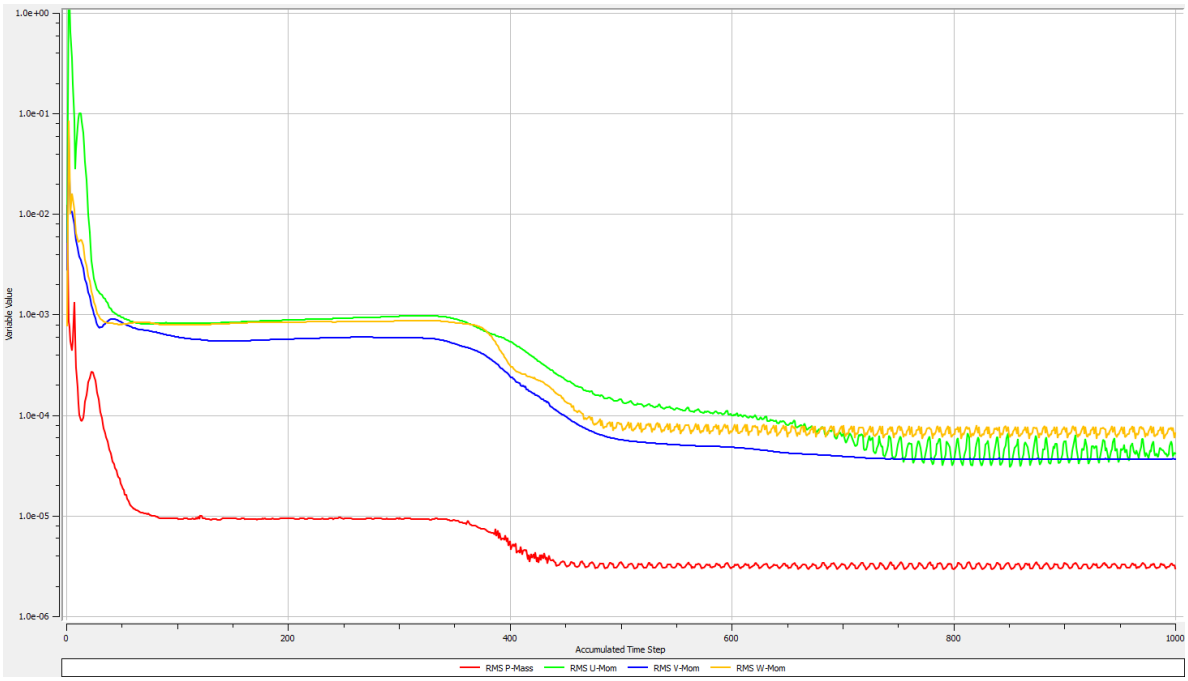

Figure 4. 9: residual plot of 0.45 J open water simulation

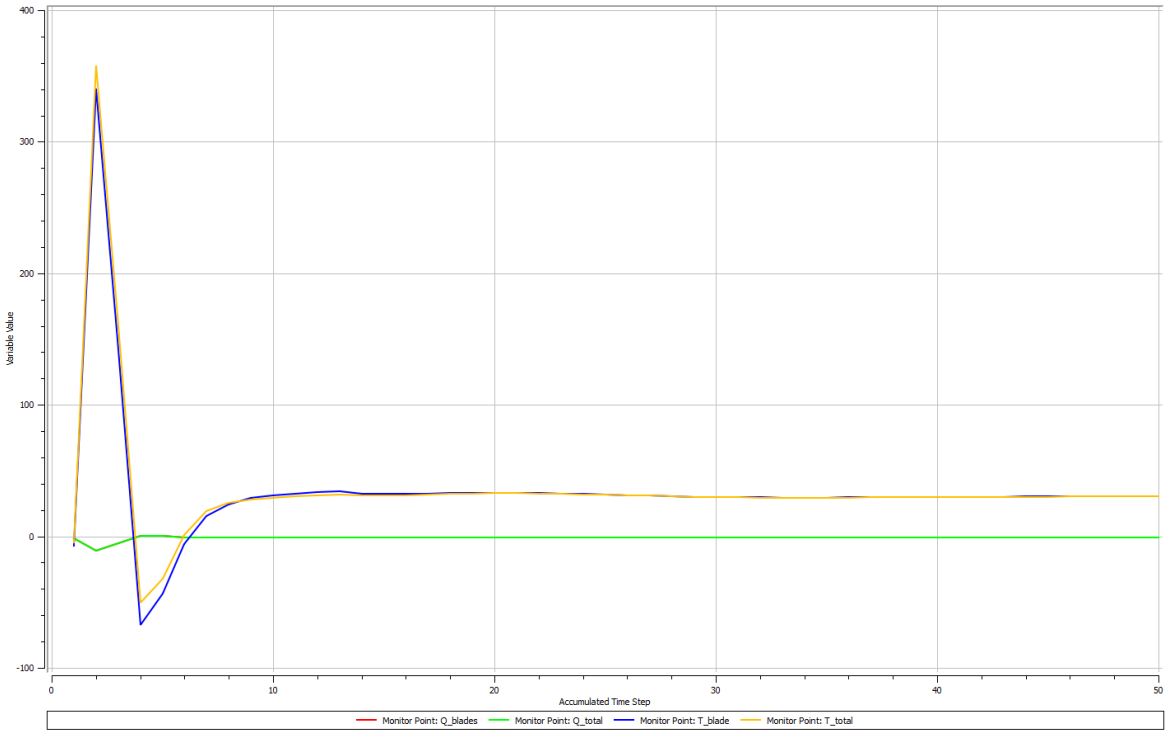

Figure 4. 10: force history of 0.45 J open water simulation

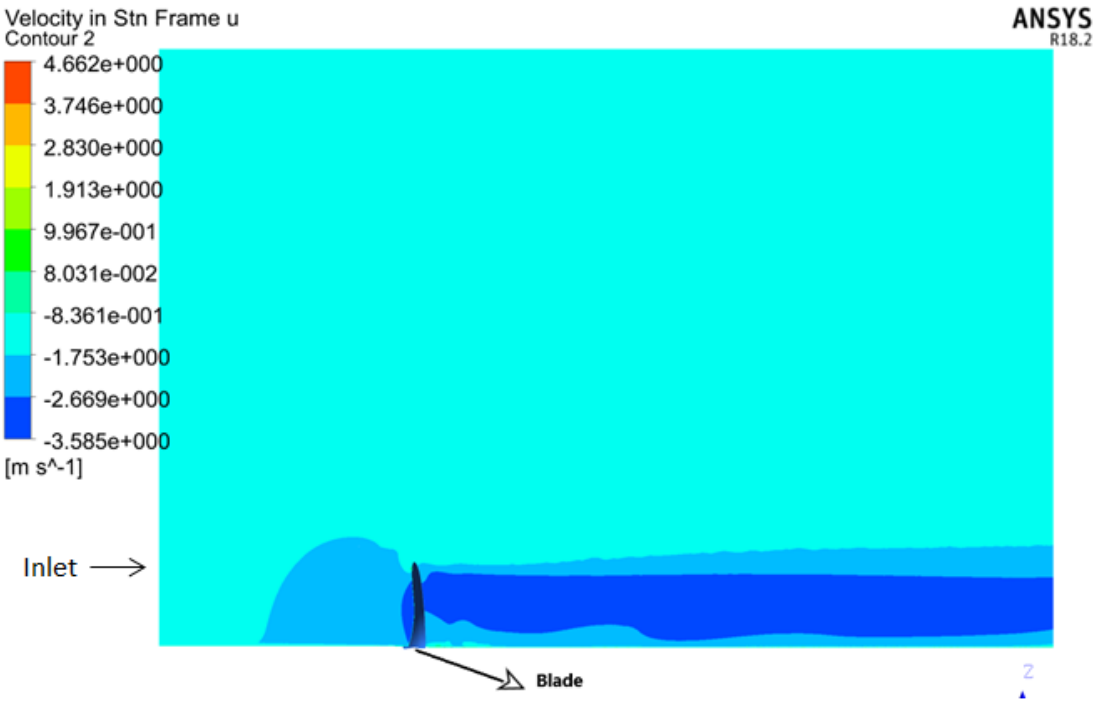

Figure 4. 11: velocity contour in x-direction

In figure 4.11, gennerally the pressure outlet condition requires the propeller influenced velocities to be zero in, but the stability of the solution is not affected and convergence is achieved with respect to both residuals and force history.This shows that a smaller domain of this size could give stable and good results. The open water test produced the following results (Table 4.3)

J	**KT**			**10KQ**			**Efficiency (η_o)**		
	Exp	Sim	Error (%)	Exp	Sim	Error (%)	Exp	Sim	Error (%)
0.45	0.206	0.196	4.70	0.265	0.256	3.36	55.766	54.932	1.52
0.50	0.185	0.176	4.85	0.246	0.239	3.28	59.804	58.771	1.76
0.55	0.163	0.156	4.76	0.227	0.220	3.11	63.079	61.944	1.83
0.60	0.141	0.135	4.43	0.206	0.200	2.85	65.442	64.329	1.73
0.65	0.118	0.113	3.74	0.183	0.179	2.62	66.502	65.691	1.23
0.80	0.042	0.0429	3.11	0.104	0.1035	0.45	51.029	52.852	3.45

Table 4. 3: Results of open water test

It can also be noted that the error is higher at lower J value; this could be due to laminar flow existing at lower J value and failure of K-ω SST model to capture the laminar effects. This analysis is consistent as at higher J values the errors are lower.The main aim of this study is to determine the necessary mesh refinement as reference for further work in a much reduced computational resources and cost.

5 FLUID-STRUCTURE INTERACTION METHODOLOGY

The entire project is performed in ANSYS framework. The main aim of the project is to perform a fluid structure interaction for propellers. The project involves predicting the propeller characteristics and resulting forces which are to be used for structural analysis. Fluid structure interactions is coupled by a one-way coupling method. This method transfers pressure forces from hydrodynamic analysis to structural analysis but does not return the deformations for 'deformed structure' hydrodynamic analysis. A one-way coupling analysis is tried using the numerical results of Section 3. ANSYS allows internal coupling between CFX and Mechanical (ANSYS documentation version 18.2). The coupling structure in ANSYS is shown below (Figure 5.1).

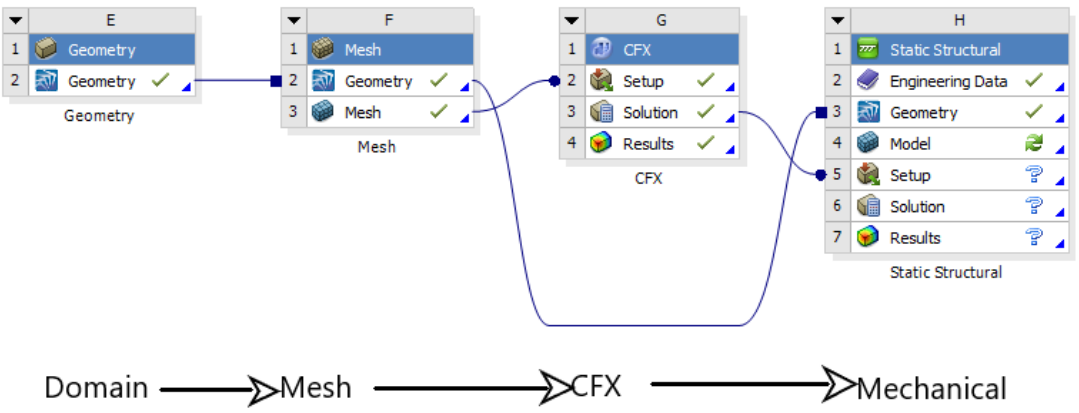

Figure 5. 1: ANSYS Frame work for FSI

The coupling procedure recommended by ANSYS revealed a very crucial weak point in ANSYS framework. The mapping of pressure which occurs internally, took a long time to transfer pressure points from CFX to Mechanical. However, when the same points are extracted from CFX as data file and imported into Mechanical as an external data file, the mapping is performed under a minute. This could be down to the complex geometry of the propeller or could be due to delay in finding nearby nodes by the internal mapping algorithm. Another major issue identified is the inability to scale. Most hydrodynamic simulations of propellers are performed in model scale and the structural analysis is performed in full scale. This is not possible in ANSYS framework as ANSYS only allows coupling at similar scale. Also, in the context of structural analysis of propellers, it is not important to find structural characteristics at all points of revolution. Only four focus points per revolution of a single

blade are of importance; Maximum thrust point, Minimum thrust point and two average thrust points per revolution. The maximum and minimum thrust points are found to estimate fluctuation and maximum load acting on the propeller. To solve all of these issues an external coupling is developed with the use of python programing. The entire procedure is shown in Figure 5.2.

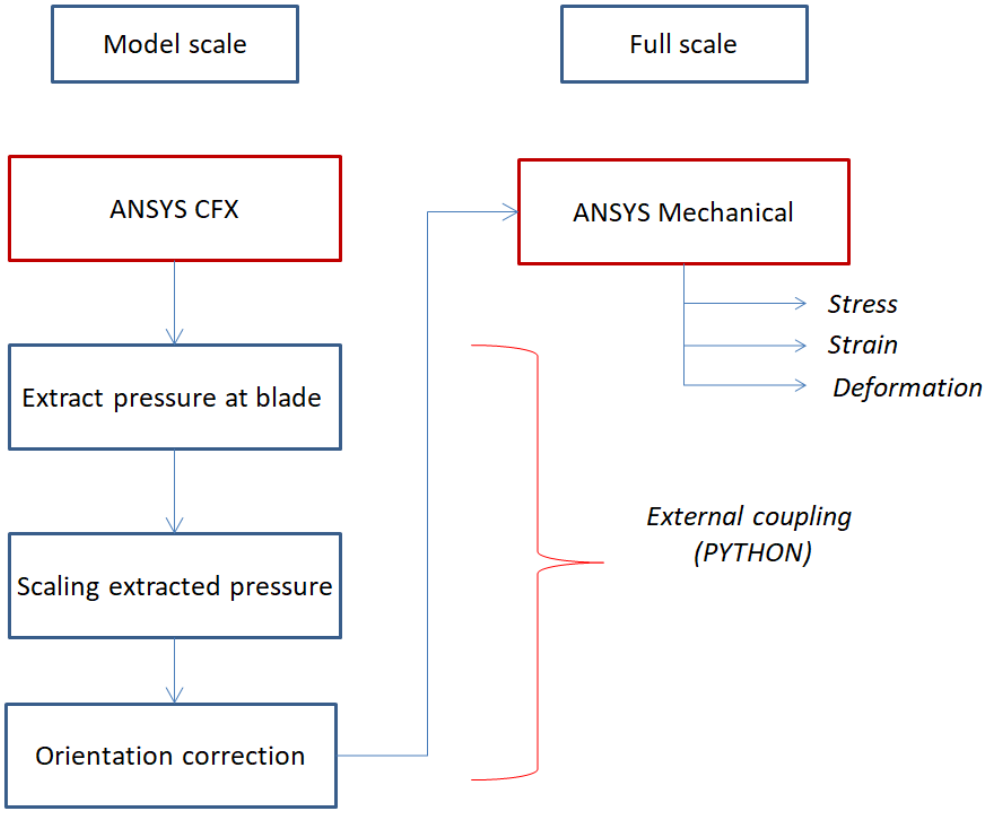

Figure 5. 2: External coupling using python program

The coupling process defined in Figure 4.2 is repeated for all four focus points. The scaling of pressure values are carried out by non-dimensionalising the pressure point by converting it into coefficient of pressure (C_p). The equation of coefficient of pressure is given below.

$$Cp = \frac{Pressure\ (P)}{0.5\ \rho\ n^2 D^2} \tag{9}$$

Since the four focus points occur at various degrees of rotation, the extracted pressure points have to be reoriented back to initial position for structural analysis.

The time and computational cost associated with Fluid-structure coupling is contributed mainly by RANSE based hydrodynamic analysis. To reduce the computational load, two levels of reduction in domain sizes have been proposed in this thesis. The reduction applied in

section 6 is a direct reduction from regular domain used in the industry for self propulsion simulation (Figure 6.1). The regular domain is applied when behind ship or self propulsion test are performed numerically.But this is unnecessary when it comes to prediction of thrust produced by the propeller especially if the propulsion point is known i.e rps of propeller and ship speed. The propeller thrust for behind ship condition only depends on the wake flow on to the propeller. This can be modelled by reducing the domain by cutting the ship near its transition from parallel middle body to length of run. It is assumed that the wake on to the propeller has very little to no influence on the shape of the fore part of the hull. Another advantage of cutting the domain to just the aft section is the elimination of the need to model the far field as far field is usually required to account for wave development and wave dampening in the domain. Therefore, similar far field distances as that of open water simulation (Section 4) is only required to be added to domain aft of the ship. Taking all this into consideration, the first level of reduction is proposed which reduces the regular domain to a much smaller and focused domain for behind ship thrust prediction for propellers (Figure 6.2 and 6.3) if propulsion point is known .The results and discussions are available in Section 6 and 7.

The second level of reduction is for further simplification of behind ship thrust prediction. The simplification proposed in Section 8 uses wake as inlet.The method of simplification of behind ship condition using wake as inlet has been around for some time. Since nominal wake field can be provided by model testing facilities and also found numerically with relatively low computational cost, this method gives good flexibility. However, the standard domain cylindrical domain used for this analysis is shown in Figure 8.1. An investigation into the effectiveness of this domain revealed two major faults. The major fault is the dilution of wake contours as it propogates along the domain due to velocity gradient. This creates a situation where the propeller has to be kept close enough to the inlet to achieve proper inflow.The proximity to inlet revealed subsequent fault. The proximity to the inlet means that suction created by the propeller cannot be fully developed as the inlet velocities in numerical analysis stays constant at inlet boundary. This meant a modification to the domain had to be proposed to get accurate results. The detailed analysis and the proposed solution to both the analysed faults are mentioned in section 8. The proposed modification to the standard domain shows faster convergence of forces and reduction of computational cost with good accuracy of results. The modfied domain can also be used for cavitation simulation as well.

6. BEHIND SHIP CONDITION

The self-propulsion test is performed on the ship and propeller defined in section 3. The ship is run at operational condition OCB 1 and OCB 2.

6.1 Numerical estimation of self-propulsion test

The standard domain used for behind ship simulation is similar to resistance test where a part of the towing tank is used as a domain (Figure 6.1).

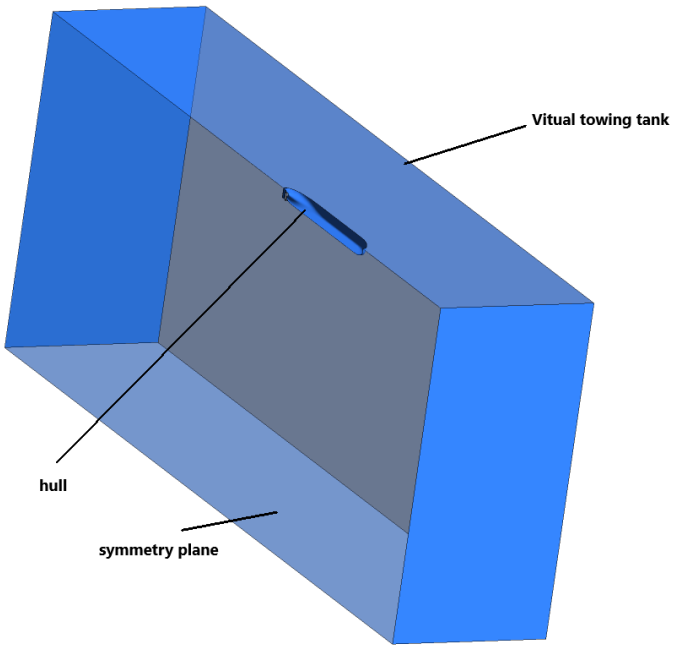

Figure 6. 1: Resistance test domain

But this requires meshing a lot of region which is not necessary for propulsion simulation and thus results in unnecessary computational cost. Therefore a significantly reduced domain is proposed to simulate the propulsion test (Figure 6.2 and Figure 6.3). The reduced domain is proposed under the assumption that wake from the ship can be adequately captured using this reduced domain. The depth of the domain is decided to simulate deep water condition and therefore, a depth of draft(T)/Depth(H) of value greater than 2.5 is applied (shallow water, T/H <= 1.5). Since no waves are simulated side walls are defined close to the domain as wave reflection is avoided. The far field distance similar to open water condition decided to outlet distance from propeller. These assumptions are proved to be accurate as you will see from the results in this section.Thrust identity point is not used here as this simulation is direct comparison with self propulsion test done in towing tank.

6.2 Numerical setup

The single phase simulation with fluid medium as water at 997 kg/m^3 density is used for simulation.Turbulence is modelled using K-ω SST. Unlike, open water test, a transient analysis is required for this simulation as inflow on to the propeller is non-uniform and hence thrust at each degree of rotation is different. Similar to open water simulation two domains are required to perform behind ship condition. The inner domain is given a constant rotation rate to simulate propeller rotation while outer domain can remain as stationary domain to simulate flow around the vessel. The domains used are shown Figure 6.2, Figure 6.3, Figure 6.4 and Figure 6.5.

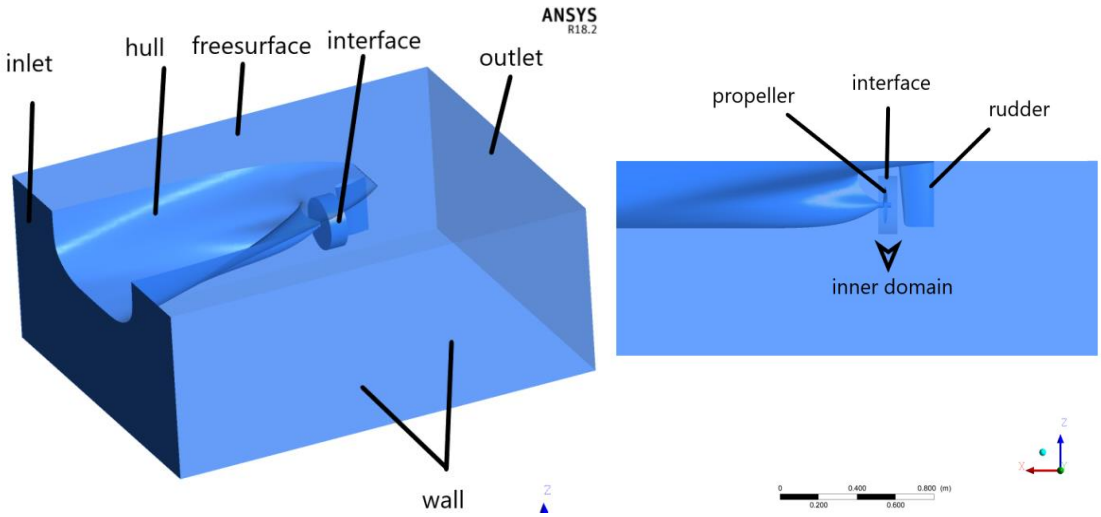

Figure 6. 2: Inner and outer domain

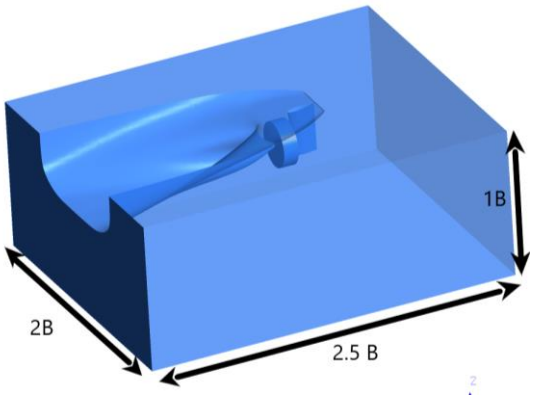

Figure 6. 3: Outer Domain dimension

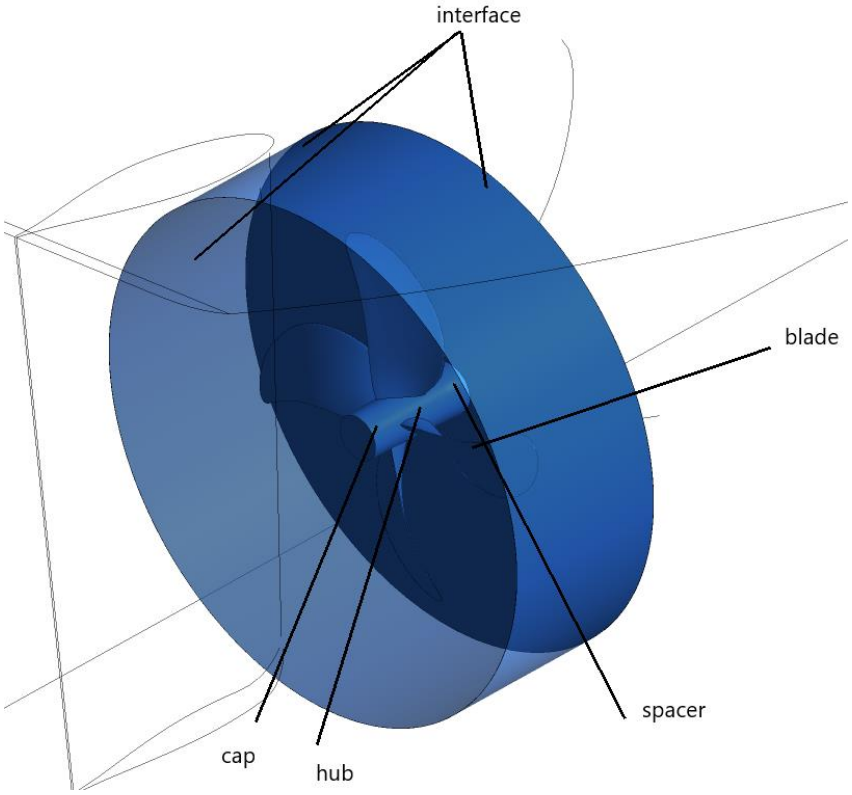

Figure 6. 4: inner domain boundary conditions

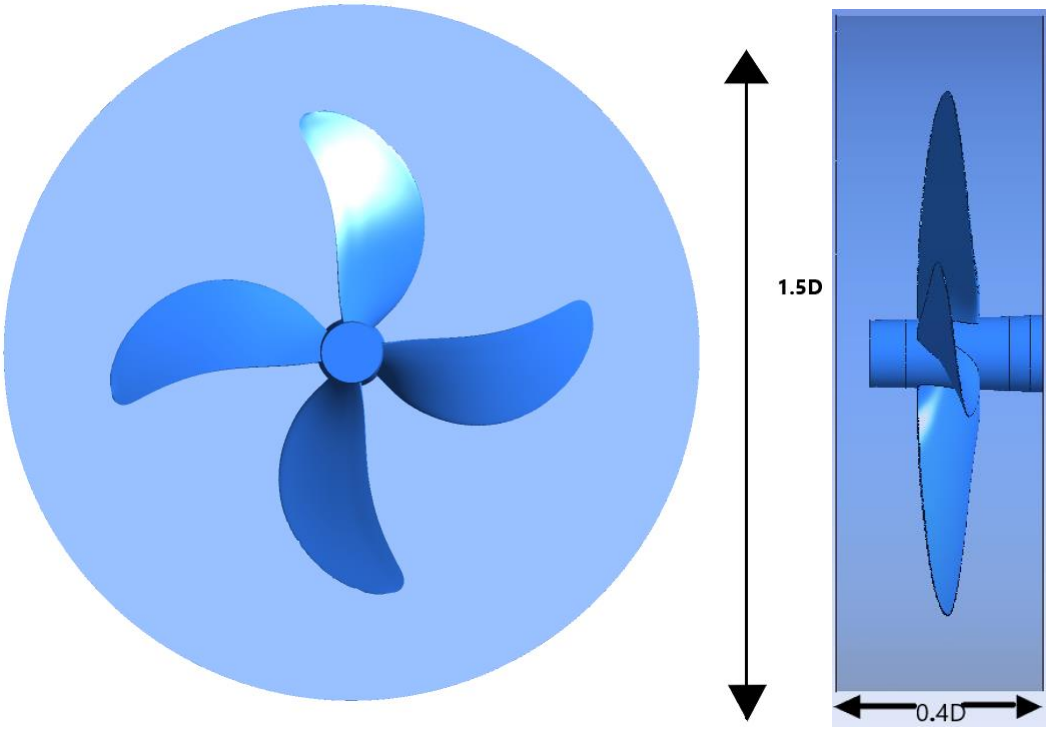

Figure 6. 5: Inner domain dimensions

The applied outer domain boundary conditions are shown below (Table 6.1):

Boundary	condition
Free surface, side and bottom wall	Free slip wall
Hull and rudder	No slip wall
inlet	velocity inlet
Outlet	pressure outlet
interface	Transient rotor

Table 6. 1: Outer domain boundary conditions

The inner domain boundary conditions are shown below (Table 6.2):

Boundary	condition
Interface	Transient rotor interface
Blades , hub , spacer and cap	No slip wall

Table 6. 2: Inner domain boundary conditions

All free surface effects at the interface between water and air are not considered for this simulation since the propeller is at sufficient depth and propulsion point is already known. The inlet velocity and propeller RPS are given the same values as OCB1 and OCB 2.Since, the analysis is performed in transient condition, a timestep has to be defined. Time step is the incremental change in time for which the governing equations are being solved. For propellers, it is most commonly identified as the increment in time per degree of rotation as the timestep. As the timestep gets smaller the fluctuations in forces are more aptly captured. But smaller timestep means more number of iterations are required per simulation. Also, in case of propellers, a lot of water has to be “pushed” to reach a converged solution. This means at small timesteps, the simulation has to run for a much longer time to reach convergence. Therefore, to avoid this problem a changing timestep is defined. A stepping function is used to facilitate this change with time step becoming smaller and smaller as the number of steps increases. At initial stage the time step is chosen to simulate 50 degrees of rotation per time step and eventually reduce it down to 5 degrees per time step.

6.3 Mesh generation and Mesh dependency

The inner and outer domains are meshed separately. The outer domain is meshed with refinement determined by proximity to the hull and rudder surface. A volumetric refinement is provided at the aft of the ship to effectively capture wake of the ship coming on to the propeller. For the inflation layer the first layer thickness of the mesh is given a value suitable to ensure that the wall Y+ is above 30 and also number of layers are controlled to ensure smooth transition from inflation layer to outside mesh. Tetrahedral mesh is used for meshing (Figure 6.6).

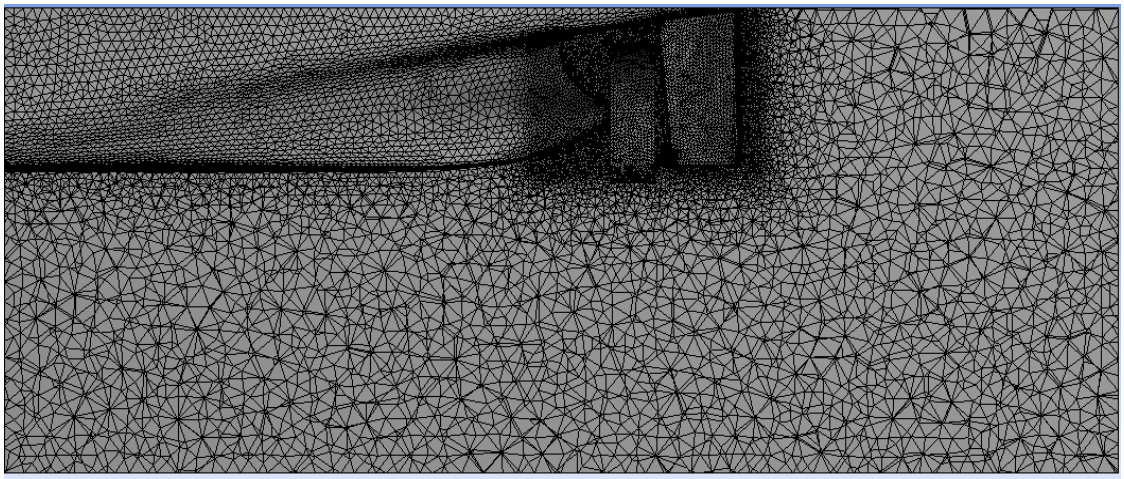

Figure 6. 6: Outer domain mesh

The inner domain is also meshed with tetrahedral cells. Refinements are provided for each blade surface to ensure capture of propeller geometry, especially at the leading and trailing edges. Inflation layer is controlled to ensure a Y+ value above 30 and also smooth transition (Figure 6.7).

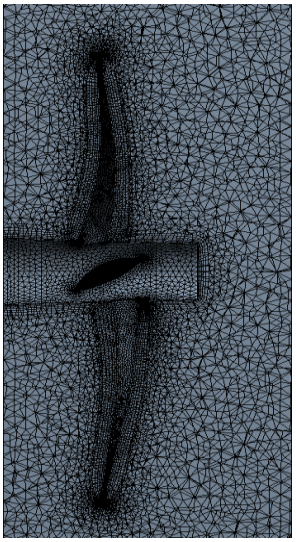

Figure 6. 7: Inner domain mesh

Mesh is given similar refinement to that of open water test. The only difference in mesh settings are the number of inflation layers assigned. Since the open water test is carried out at Y+ < 1 , the number of inflation layers required to achieve smooth transition to outside cells are very high, resulting in very high number of cells. To reduce the number of cells the Y+ is aimed to be above 30 such that wall function can be applied, thus reducing the number of inflation layers required for smooth transition and also computation cost. This resulted in 15 layer reduction of inflation layer and reduced the number of cells.

6.4 Results and discussion

The residuals are the first indication of convergence of the solution.

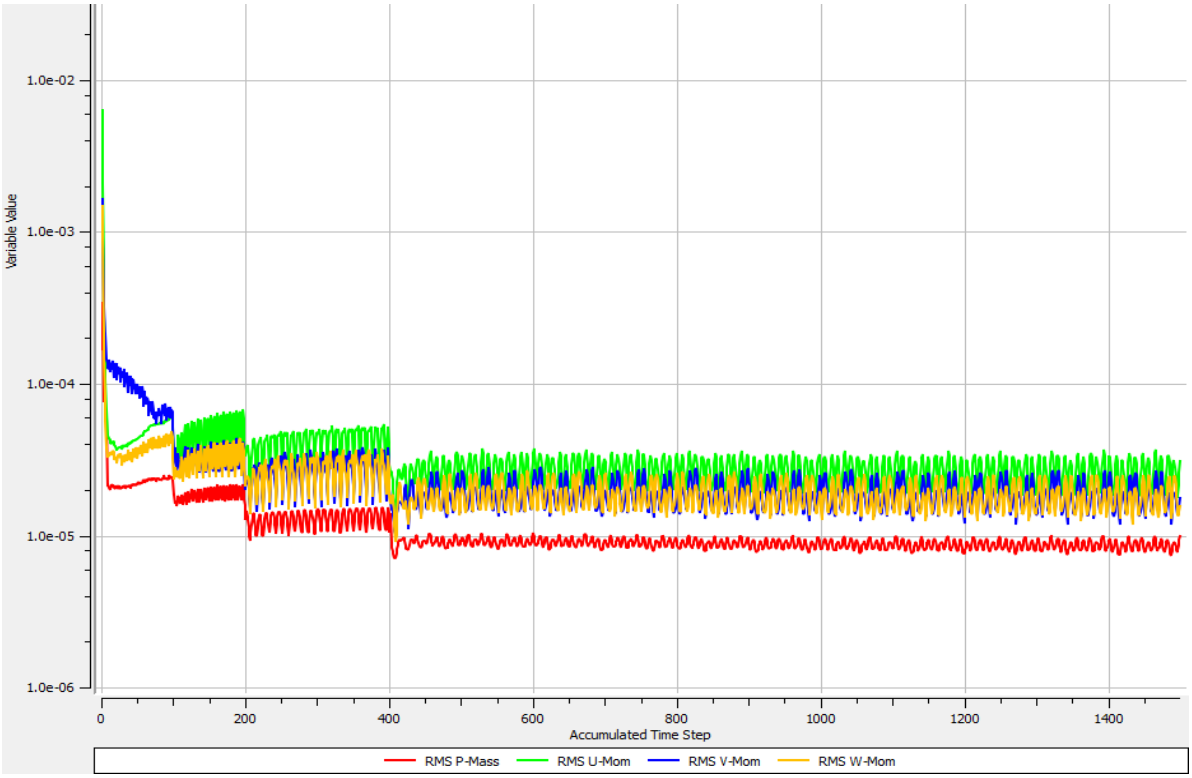

Figure 6. 8: residual plot of behind ship condition in model scale

Figure 6.8 shows the residual plot of self-propulsion simulation in model scale.The low value of residuals indicates towards a convergence of forces. The sharp drop in residuals at various points is indicative of the stepping function reducing time step. The reduction in timestep is associated with a lowering of residuals value which also indicates that there are lower fluctuations between iterations as timestep reduces. Although residuals indicate towards a convergence of the solution, force convergence also has to be checked to ensure convergence is achieved.To ensure proper capture of boundary layer and save computation time, Y+ is kept

above 30 (Figure 6.9).The difference in Y+ contours on each blade is the result of ship wake effecting inflow onto the propeller blade resulting in each blade experiencing different velocities at each position of rotation.

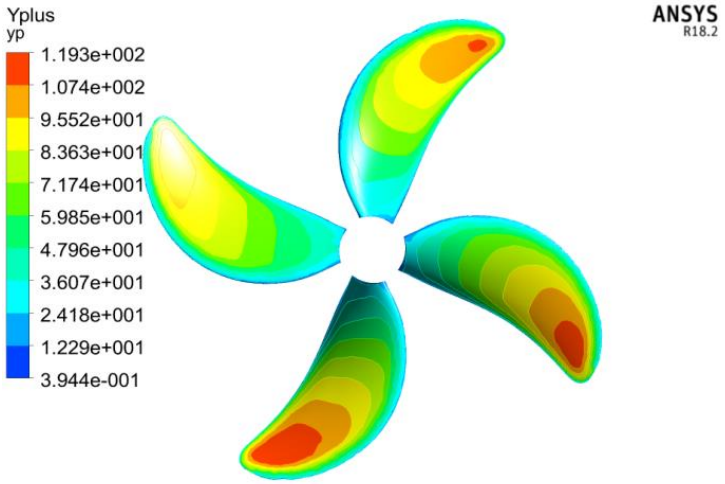

Figure 6. 9: y+ of propeller

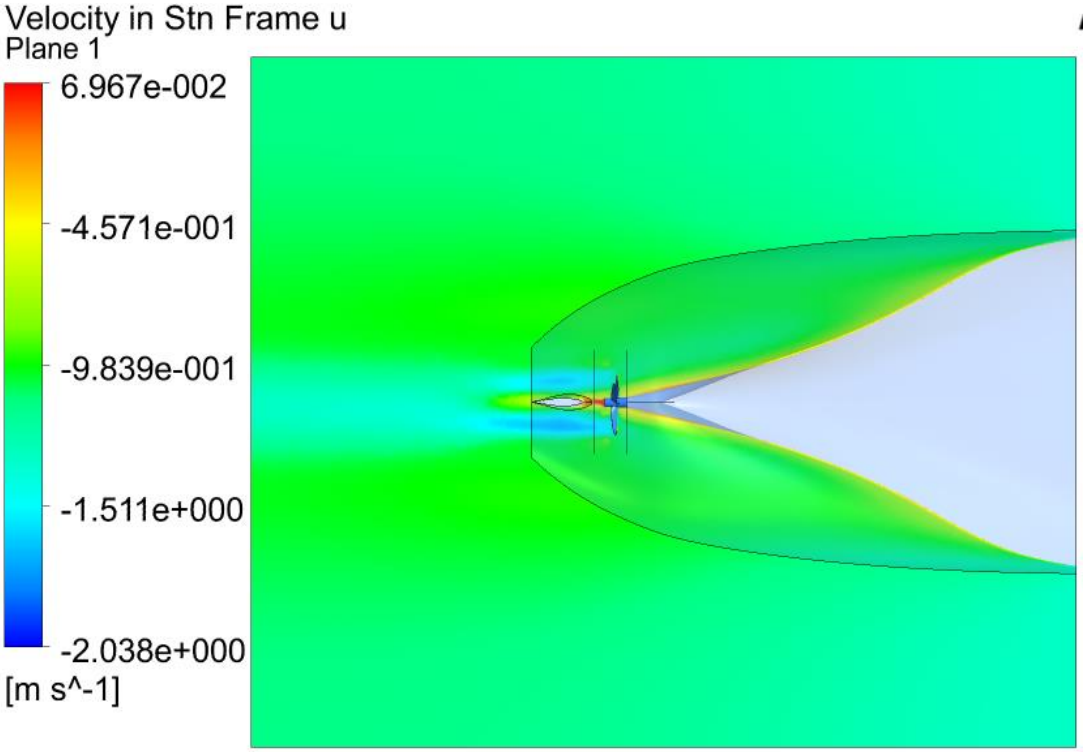

Figure 6. 10: Velocity contour cut at shaft axis in XY plane for model scale

The velocity contour in x direction (Figure 6.10) shows the increase in velocity due to the action of propeller. If noticed carefully the effect of wake of the ship existing to a high extends around the propeller can be seen.

The thrust history of a single blade of propeller in model scale and full scale are shown in Figure 6.11 and Figure 6.12. Each time step (X axis) corresponds to about 5 degrees of

rotation.The sinusoidal wave shaped curve is obtained because of the influence of the effective wake acting on the propeller (Figure 6.14). The non-uniform inflow onto the blade results in different thrust being produced for each degree of rotation. Between the two thrust histories the general shape of the curves are similar. But there exist a noticeable local maxima in thrust between two successive maximum points for full scale results which is absent in model scale results. The absence of these local maxima in model sale results could be due to time step. In both cases the final time step corresponds to 5 degree of rotation per time iteration. But this might not be enough for model scale and a further reduction to lower time step such as 1 or 2 degree per time iteration could be required. This kink in value could also be due to the difference in contours of effective wake acting on the propeller (Figure 6.14). The model scale wake has a larger portion of very low velocities compared to full scale wake but more importantly the transition from low velocity region to high velocity is much smoother in model scale which leads to a smoother thrust curve. A further investigation by lowering time step could be performed to identify if the kink is also present in model scale. But, as the fluid-structure coupling looks for structural characteristics only at 4 focus points per revolution, the thrust history shows that these focus points are not affected by the kink in value. The lines of interests are marked in figure 6.11 and figure 6.12. The points for structural evaluation are performed at the points of intersection between the thrust curve and interest lines.

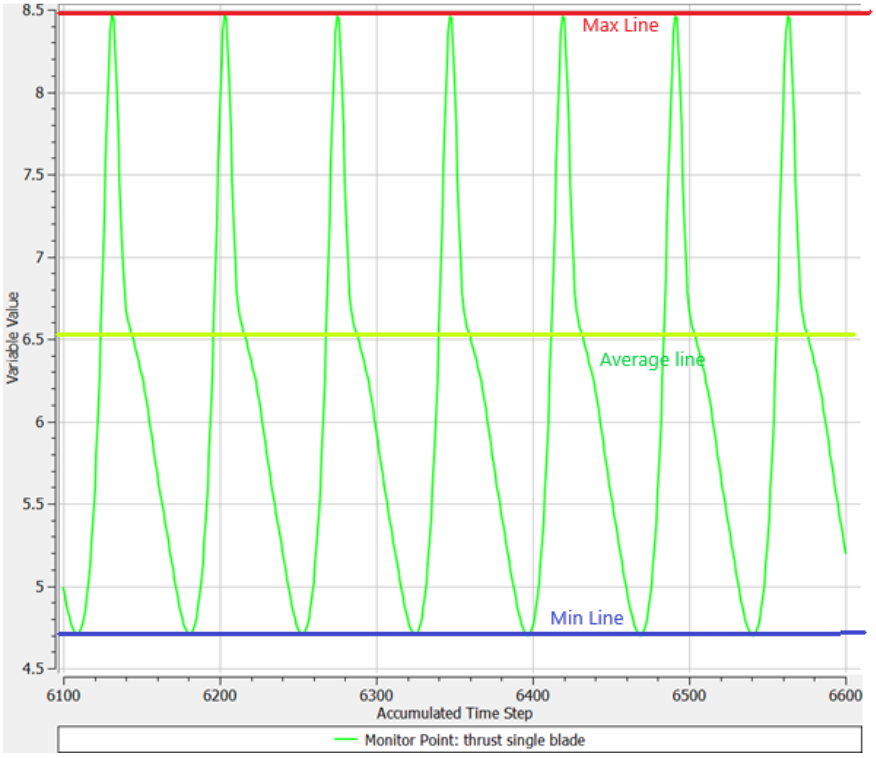

Figure 6. 11: Thrust history of single blade

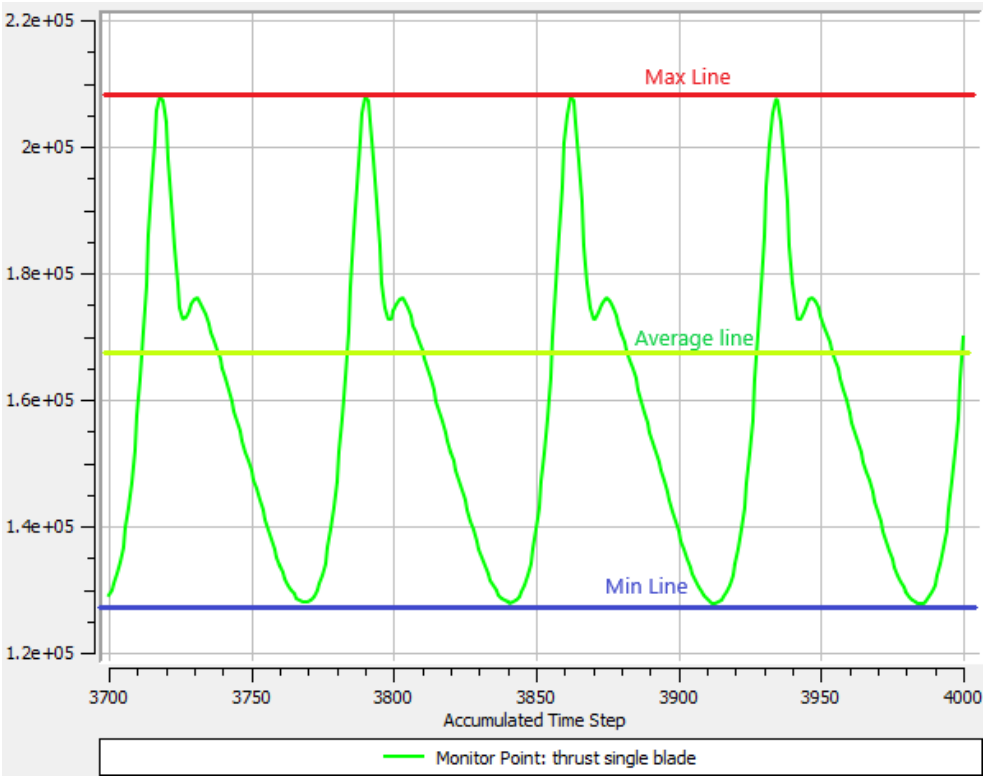

Figure 6. 12: Thrust history of Full scale propulsion test

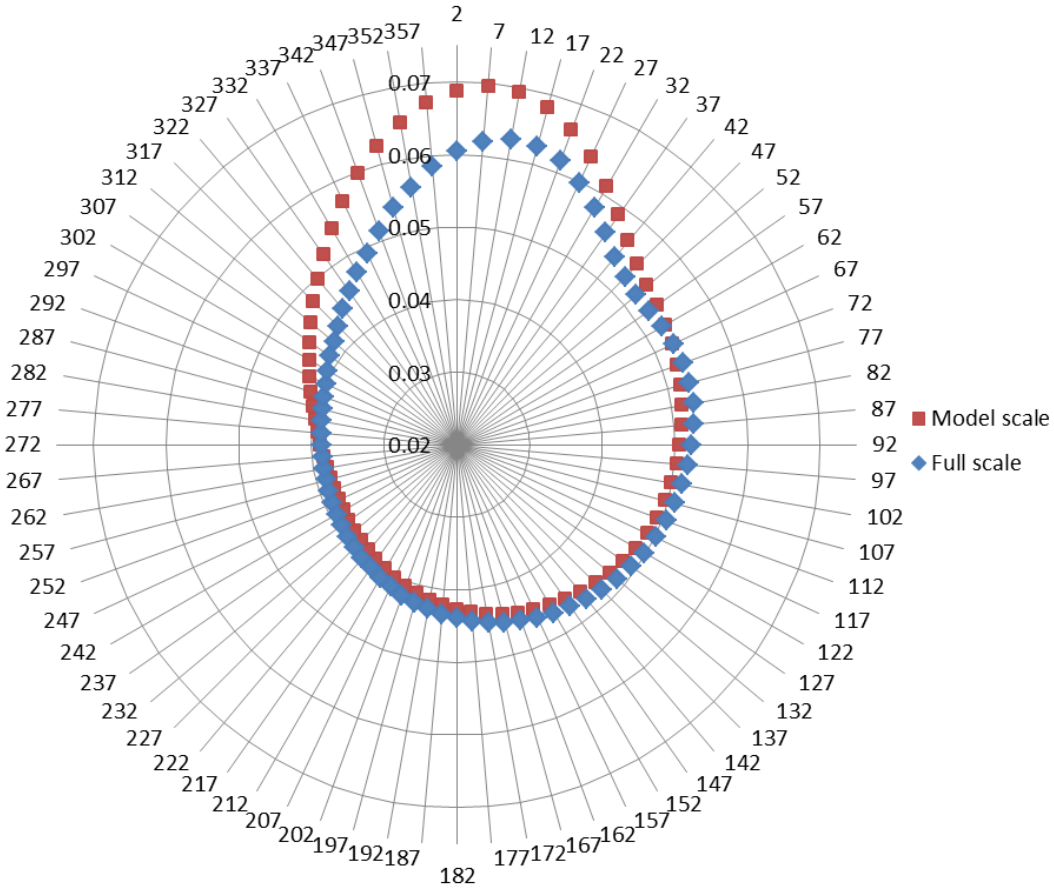

Figure 6. 13: Shows thrust history in terms of K_T at each angle of rotation

Further investigation into thrust history comparison (Figure 6.13) at each angle of rotation indicates that the thrust history at full scale does have an increase in value midway as it transition from maximum thrust point to minmum thrust point . While model scale shows a smooth transition from maximum thrust point to average point.It could be deduced that the previous assumption of timestep causing the missing of kink in value is invalid.This can then only be caused by wake differences shown in figure 6.14.

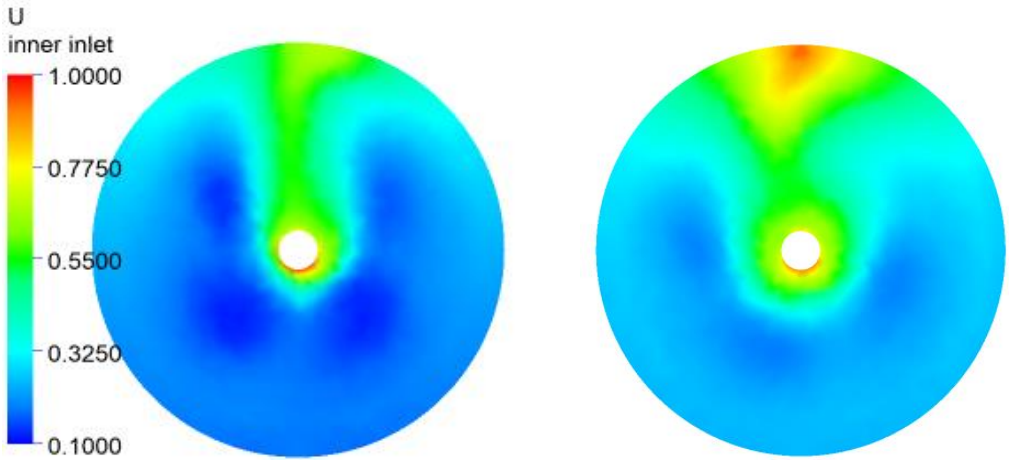

Figure 6. 14: Effective wake in full scale(left) and model scale (right) in terms of wake fraction

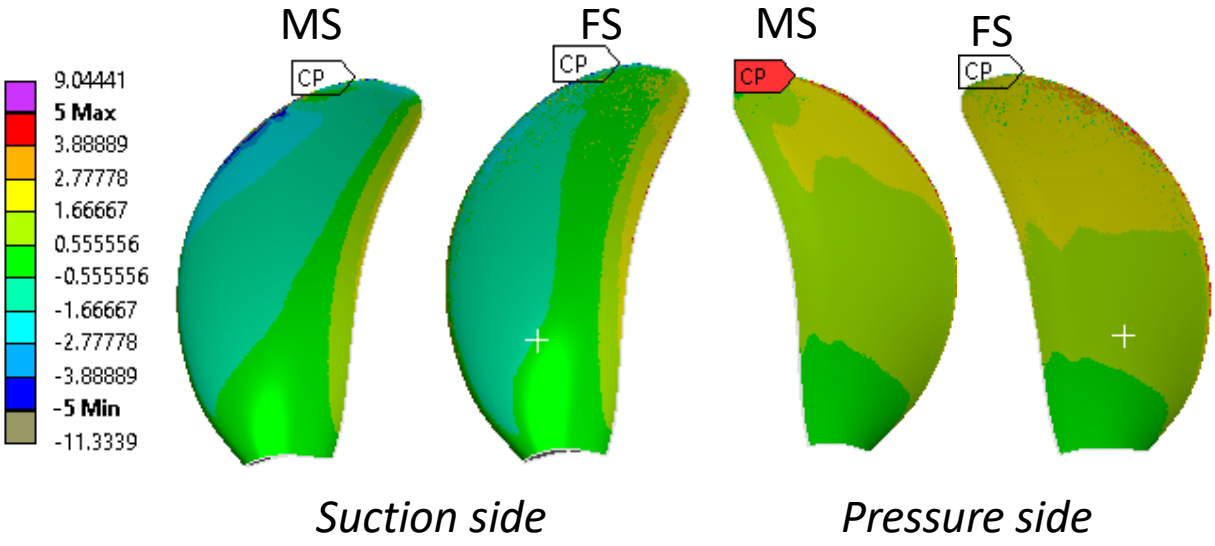

Figure 6. 15 :Pressure distributions in terms of Cp in model scale (MS) and full scale (FS).The scale has been adjusted to show difference in contour

It can be noticed that the wake profiles are different. The change in velocity profile leads to difference in thrust and torque developed on the blades as it rotates. A narrower region of slower velocity (higher wake fraction) and subsequent abrupt change to higher velocity region

in the case of full scale wake could be the reason for sharp drop in thrust and a kink in value. A wider region of low velocities could be the reason for smoother transition in case of model scale wake. This is expected as boundary layer effects are dominant in model scale results.

This change in wake profiles also changes the pressure distribution on the blade profile. Figure 6.15 shows the difference in pressure distribution in terms of Cp at maximum point of thrust. It can be observed that at the pressure side the distribution remains almost identical. But, the model scale has higher pressure values near the tip at leading edge. This shifts the centre of pressure towards the tip creating addition moment and hence bending stresses. And similarly , for the suction side it can be observed that higher pressure exist more consistently along the radius of the blade at trailing edge. This reduces the overall thrust developed at trailing edge. And also, the leading edge of suction side in model scale shows very low pressure, which also leads to centre of pressure moving up towards the tip of the blade.

The resulting total thrust and torque acting on the propeller and its comparison to experimental results are shown in table 6.3.

	Thrust (N)	Torque (N.m)	K_T	Error (%)	$10K_Q$	Error (%)
Full scale	632955	527745	0.191	1.59	0.253	9.14
Model scale	23.50	0.656	0.192	1.64	0.255	9.89
Experimental	23.13	0.597	0.188		0.231	

Table 6. 3: comparison of model scale vs. full scale vs. experimental results

The results show good agreement with experimental results, which indicates that the initial assumptions are correct. This domain could be used to get accurate results if the propulsion point is known with lower computation cost

7. FEA ANALYSIS OF BEHIND SHIP CONDITION

As mentioned in Section 5, a python program is used to extract the pressure points from ANSYS CFX and import the same pressure points to ANSYS mechanical for FEA analysis.For performing the FEA analysis four points are of interest (Section 5). Since, the thrust history shows a sinusoidal wave pattern, for a design point of view, the maximum point, minimum point and two average points in one revolution are considered as key points of FEA analysis. The two average points are of concern as pressure points acting on the blade will not be the same due to difference in wake even though the overall forces remain similar.. The main aim of the analysis is to compare structural between the results obtained from scaled pressure of model scale vs. the directly obtained pressure values of Full scale CFD analysis.

7.1 Geometry

A single blade at full scale is used for FEA analysis. The geometry is shown in Figure 7.1.

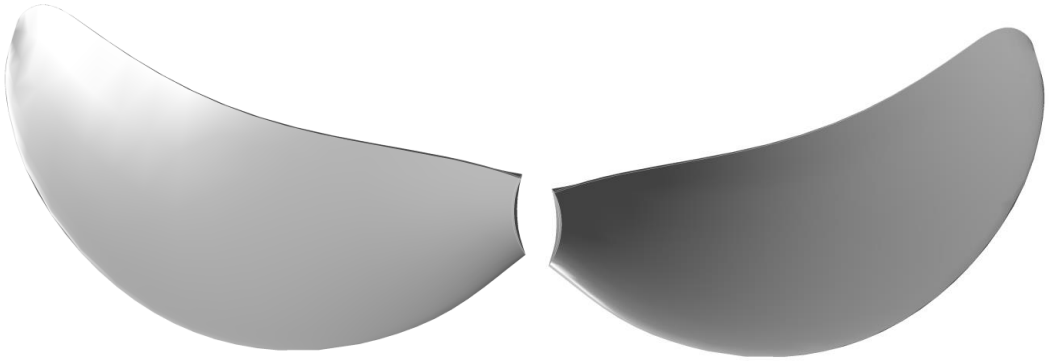

Figure 7. 1: Geometry of single blade

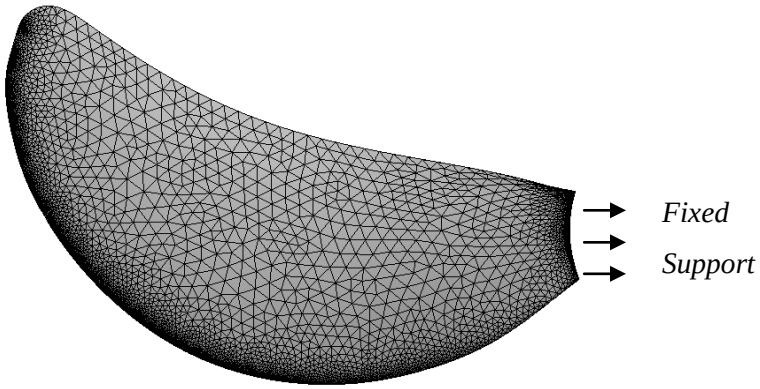

Figure 7. 2: Mesh used for FEA analysis and fixed support location

7.2 Mesh

The mesh developed for FEA analysis is shown in Figure 7.2.A tetrahedral mesh is used to mesh the geometry. A refinement based on curvature of the blade is applied to refine the leading edge of the propeller blade. This is done in accordance with the similar refinement applied on the blade for CFD analysis to ensure much faster and proper mapping of pressure points and also allow enough refinement at the root of the propeller where maximum stress is predicted to concentrate as the blade is effectively a cantilever beam.

7.3 Analysis setup

The analysis is setup with the propeller blade being analysed as a cantilever beam. To reduce the computation cost only one blade is used for analysis with the root of the blade given a boundary condition of fixed support (Figure 7.2).The pressure from CFD analysis is mapped onto the FEA mesh. Two sets of CFD pressure are mapped and compared per focus point. The scaled model scale CFD pressure and full scale CFD pressure points.. A sample of pressure points applied on geometry and the resulting mapped pressure is shown in Figure 7.3 and 7.4

.

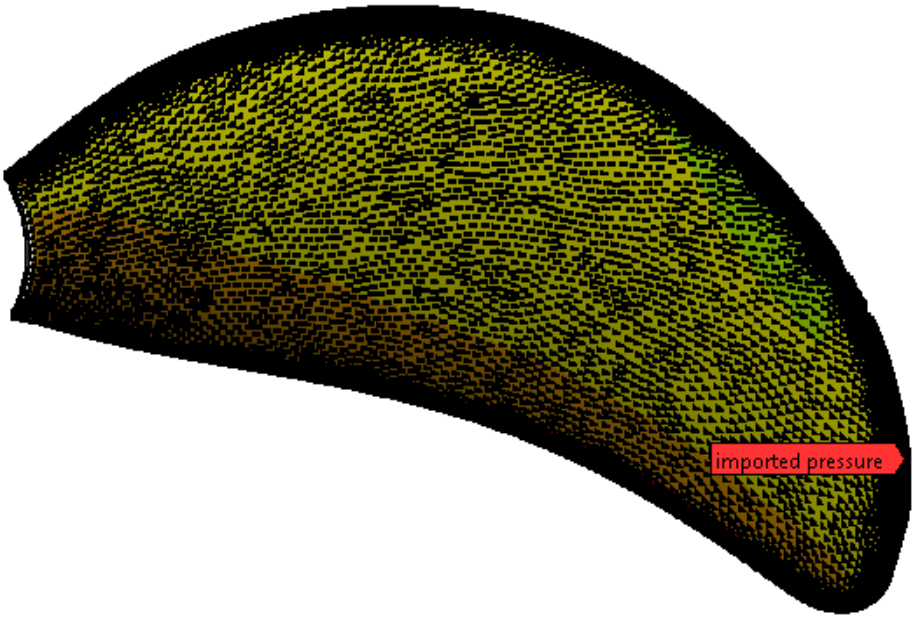

Figure 7. 3: Imported pressure points from CFX

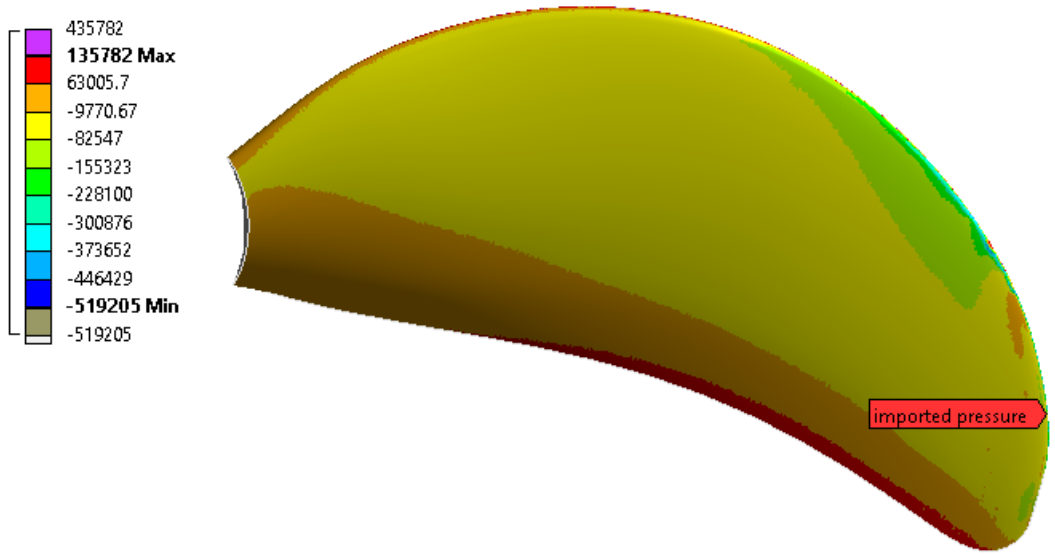

Figure 7. 4: Mapped pressure from CFX

The mapping of pressure points uses triangulation approach which will find the nearest node to the pressure point and then interpolate between the points. The solver applied a direct approach rather than an iterative approach to solve the FEA analysis to save computation time, therefore the process only considered one step. The material used to design the propeller is an isotropic alloy of Copper known as CuAl10Ni F650.The material properties are shown below in Table 7.1

Properties	Value	units
Density	7510	kg/m3
Tensile Yield strength	270	MPa
Tensile Ultimate strength	650	MPa

Table 7. 1: Material properties

7.4 Results and discussion

The main objective of the FEA analysis is to determine the Von Mises stress, total deformation and the equivalent strain associated with the load acting on the blade. As fatigue analysis is not performed on the blade, principle stresses are not of major concern for this study. It is to be noted that for the design of the propeller, the maximum allowable stress is 85 MPa. Some stresses are above the maximum allowable stress values but that is expected as the assessed geometry is modeled for CFD analysis. The geometry of the blade is usually

thickened and filleted at the root to reduce stresses. Therefore the geometry of the blade needs to be revised to meet the design criteria.

The contours shown in Figure 7.5 corresponds to scaled model scale pressure FEA analysis on the left and full scale pressure FEA analysis on the right. The contour shows good similarity between the two results. The maximum stress is also located near the root of the propeller blade. This is expected as the blade is a cantilever structure. The maximum deformation on the blade is 2.7 cm for a propeller diameter of 6 m. This could indicate that the performance of the propeller may not be affected but a detailed 2 way coupled Fluid structure interaction study has to be performed to determine the effect.

Table 7.2 considers the stress, strain deformation, and reaction forces of 4 focus points. The maximum and minimum values at each focus points are shown along with errors. It could be observed that the values having largest differences are minimum values across all focus points. But these points are not of much concern as a design point of view as maximum values are of more concern.

The maximum values at maximum thrust point is of concern as maximum stresses occur at this point. At maximum thrust point, the stress is overestimated for scaled model scale CFD results. This means that a conservative result is obtained which is good for a design point of view. The error value of less than 10% also indicates that scaling using Cp is reliable and accurate.

The two average points shows differences across all assessed values. This indicates that the pressure profiles acting on the blade are different even though the thrust remains the same. The low values of strain indicates a very low elongation of the propeller blade, which also can be considered as a good sign of reduced loss of propeller performance due to pressure force induced deformation. The low differences in reaction force indicate that the total force acting on the propeller are accurately mapped.

The overall quality and accuracy of results are good, which means that the scaled pressure fluid-structure coupling is a good way of estimate structural characteristics.

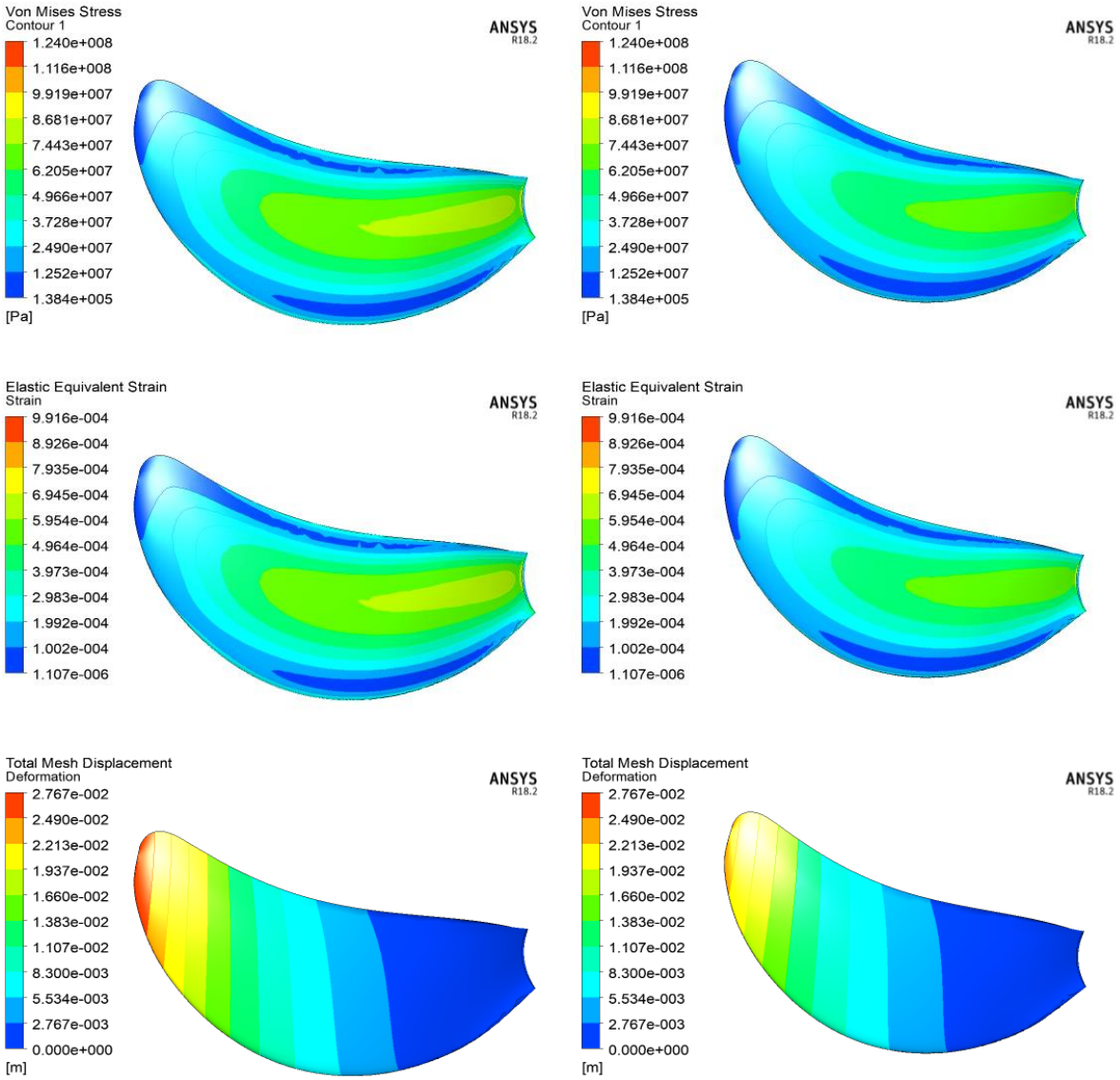

Figure 7. 5: comparison of structurally assessed values between scaled pressure FEA (left) and Full scale pressure FEA (right)

	Max Point		Min Point		Average point 1		Average point 2		
	Maximum	*Minimum*	*Maximum*	*Minimum*	*Maximum*	*Minimum*	*Maximum*	*Minimum*	
Stress(Pa)	1.240E+08	4.885E+04	7.398E+07	2.960E+04	9.831E+07	5.792E+04	9.067E+07	1.706E+04	Model scale (Scaled)
	1.140E+08	2.190E+05	8.449E+07	1.090E+04	9.947E+07	1.161E+05	9.410E+07	3.448E+04	Full scale
Error (%)	8.78	-77.70	-12.43	171.58	-1.17	-50.10	-3.64	-50.52	
Strain	9.916E-04	4.580E-07	5.922E-04	3.297E-07	7.865E-04	7.750E-07	7.263E-04	1.710E-07	Model scale (Scaled)
	9.128E-04	2.072E-06	6.768E-04	1.173E-07	7.968E-04	1.883E-06	7.537E-04	3.296E-07	Full scale
Error (%)	8.63	-77.90	-12.49	181.03	-1.29	-58.84	-3.64	-48.11	
Deformation(m)	2.767E-02	--	1.806E-02	--	2.296E-02	--	1.693E-02	--	Model scale (Scaled)
	2.356E-02	--	1.840E-02	--	2.051E-02	--	1.888E-02	--	Full scale
Error (%)	17.46	--	-1.84	--	11.97	--	-10.30	--	
Reaction force(N) (x-direction)	2.21E+05	--	1.34E+05	--	1.81E+05	--	1.60E+05	--	Model scale (Scaled)
	2.10E+05	--	1.48E+05	--	1.83E+05	--	1.74E+05	--	Full scale
Error (%)	5.61	--	-9.72	--	-0.80	--	-7.99	--	
Postion of blade (Degree)	12.5		237.5		77.5		333.5		Model scale (Scaled)
	7.5		262.5		102.5		332.5		Full scale
			Green < 10%	Orange < 20%	Red >30%				

Table 7. 2: Comparison of results of scaled pressure vs. Full scale pressure FEA analysis

8. REDUCED BEHIND SHIP CONDITION

The purpose of this study is to determine the effectiveness of a much more simplified way of simulating and assessing behind ship condition with wake as inlet.

8.1. Study of change in wake

The reduced method usually uses a wake as inlet in a cylindrical domain to simulate behind ship condition. But, the wake imported as data points into ANSYS at inlet, changes as it propagates along the x direction due to velocity gradient. The aim is to study these changes to finalise the position of the propeller so that the resulting simulation does take proper contour of wake velocity into account at propeller plane.

8.1.1 Domain, boundary condition and mesh

The domain chosen for the study is a cylindrical domain used to simulate the outer domain. The size of the domain is 3 times the diameter (D) of the propeller and 1 m in length. The domain used for the study is shown in Figure 8.1 and boundary conditions in Table 8.1.

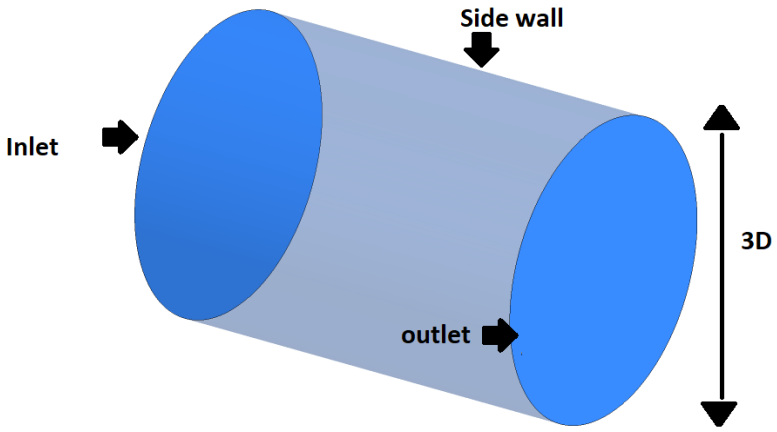

Figure 8. 1: Domain and boundary condition

Boundary	condition
Inlet	velocity inlet (wake data)
side wall	free slip wall
outlet	pressure outlet

Table 8. 1: Boundary conditions applied

The inlet boundary condition is chosen as velocity inlet. The wake data imported to ANSYS CFX module has velocity profile data points for a diameter of 300mm for a propeller diameter

of 210mm (Figure 8.2).These data points are imposed as a velocity profiles at the inlet of the domain. As the domain to be studied is much bigger (3 times the diameter of the propeller) than the available data points the values on the remaining area of the inlet is extrapolated by ANSYS (Figure 8.3).

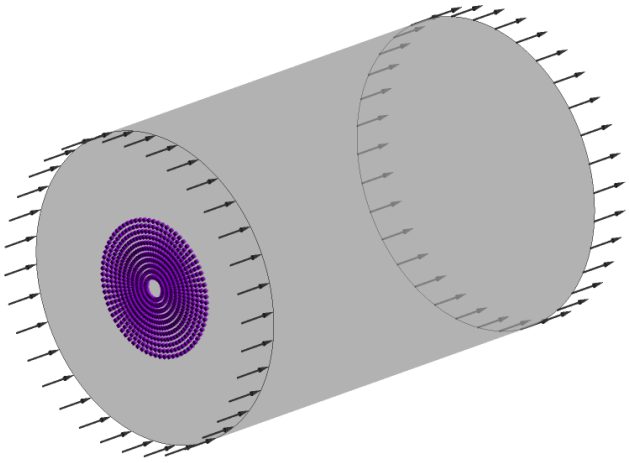

Figure 8. 2: wake as data points

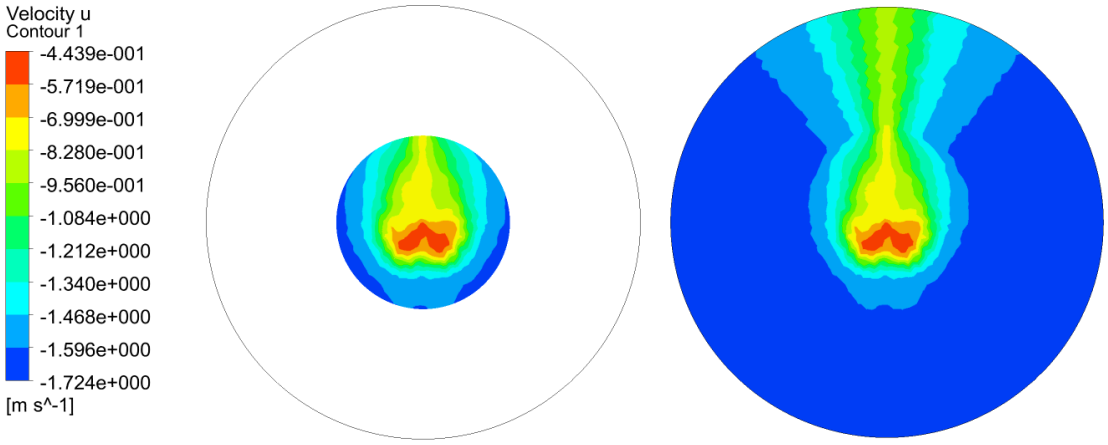

Figure 8. 3: orginial wake data (left) and extrapolated wake (right)

A uniform simple tetrahedral mesh is used with no refinement (Figure A1).

8.1.2 Result

The change is wake is studied as velocity contour in x direction (u) at 4 different distances: inlet, 0.5 D, 1 D and 1.5 D. The changes in wake obtained as evolution of wake is shown in Figure 8.4.

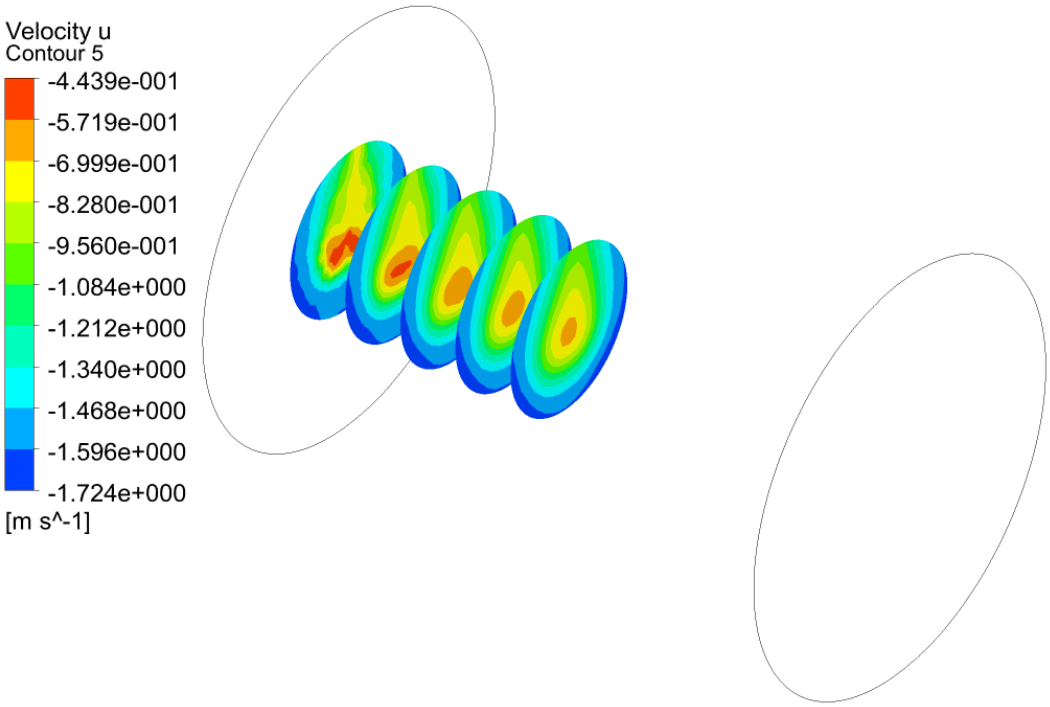

Figure 8. 4: Evolution of wake at various distances

The contour shows a rapid change in velocity profiles as well as magnitude. This suggests that in order to ensure proper inlet velocity profile of wake, the propeller should be kept within 0.5D and 0.75 D distance from the inlet at this model scale.

8.1.3 Effect of suction

The wake study shows that propeller have to be kept as close as possible to the inlet to ensure that proper wake velocity contour acts on the propeller. But keeping the propeller close to the inlet will not allow the inflow velocity to be changed due to suction of propeller as inlet velocity remains constant.. It is therefore important to study the velocity increase due to suction effect caused by propeller rotation in the domain.

In order to study the suction effect a previously simulated open water test simulation (Section 4) which is performed using piece of wedge approach is used. The simulation is performed at constant inlet velocities corresponding to different advance coefficients. The velocity at regular intervals upstream of the propeller are considered and evaluated as increase in velocity from initial inlet value. The results obtained are shown in Table 8.2 and Figure 8.5.

	J						increase from inlet value
	0.45	0.5	0.55	0.6	0.65	0.8	
location (m)	0.14	0.12	0.1	0.09	0.06	--	5%
	0.1	0.08	0.06	0.02	0.01	--	10%

Table 8. 2: location and resulting increase in velocity upstream

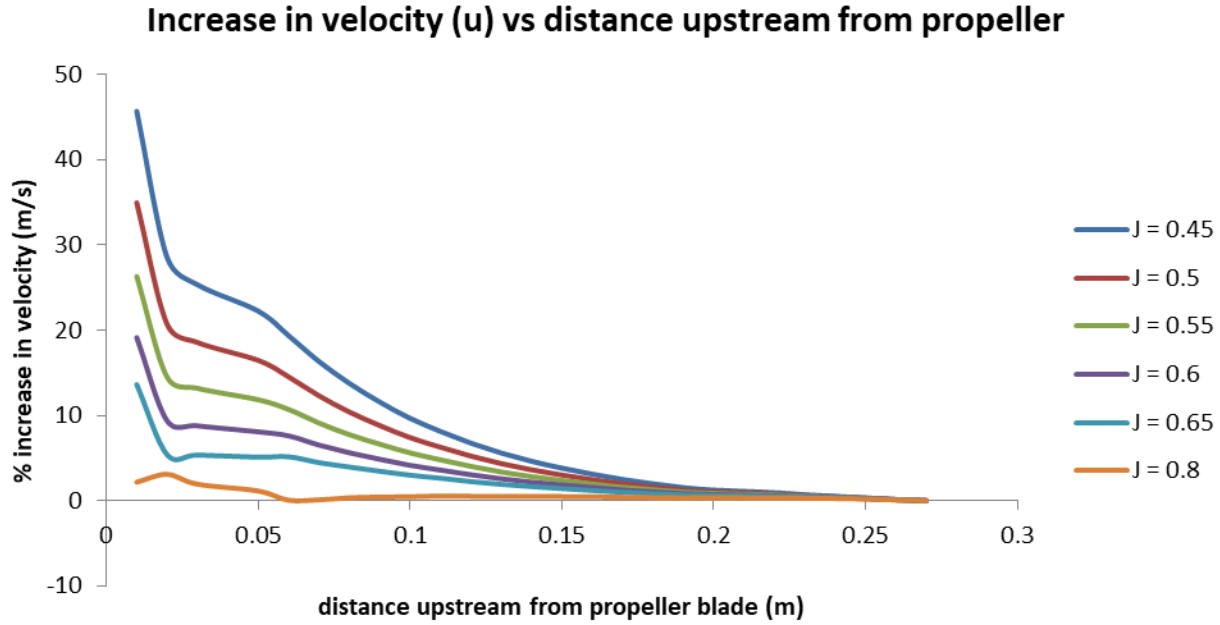

Figure 8. 5: suction induced velocity increase at various distances

8.1.4 Result and discussion

The results show that at lower advance coefficient J the suction effect is larger but effects are marginal at higher J values. The wake study showed that contour changes drastically, especially in the initial 200 mm (approx. 1 D) distance from inlet and hence indicates that propeller should be kept at a distance between 100 mm (approx. 0.5 D) and possibly 150 mm (approx. 0.75 D) for optimum wake capture. But Suction effects shows that velocity profile can be modified up to 5% at a distance of 140 mm upstream of the propeller. This could cause velocity at inlet to change. But considering lower influence of suction at higher J value and taking 10% increase as marginal, the propeller could be placed at a minimum possible distance of 0.5 D from the inlet and maximum of 0.75 D from inlet for simulating behind ship condition.

8.2 Behind ship simulation with wake as inlet

The findings in section 8.1 indicates that wake as inlet domain has some serious failings and needs to be reviewed to adequately obtain good results of behind ship condition. Therefore the domain mentioned in section 8.1.1 (Figure 8.1) is modified to solve the issues. The reworked domain is shown in Figure 8.6.

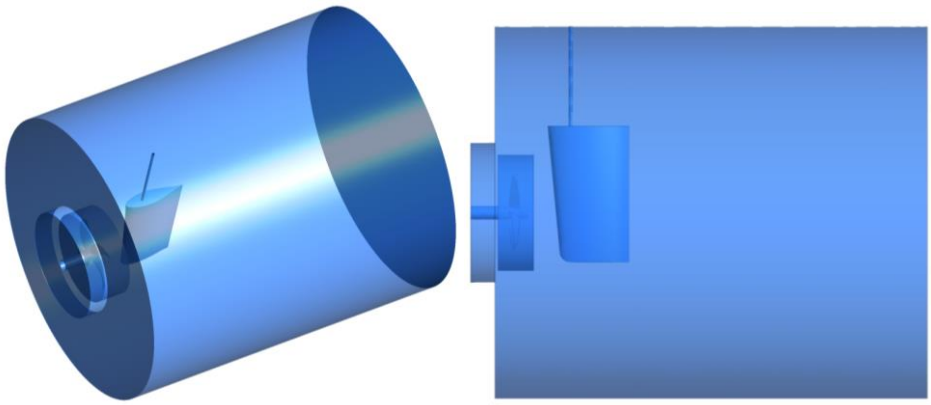

Figure 8. 6: Modified domain

The modification shows a tunnel like protrusion to the existing domain shown in Figure 8.1. This allows the wake to be kept intact by avoiding the influence of outside velocity. A simulation of tunnel and its influence on wake is investigated (Figure 8.7 and 8.8).

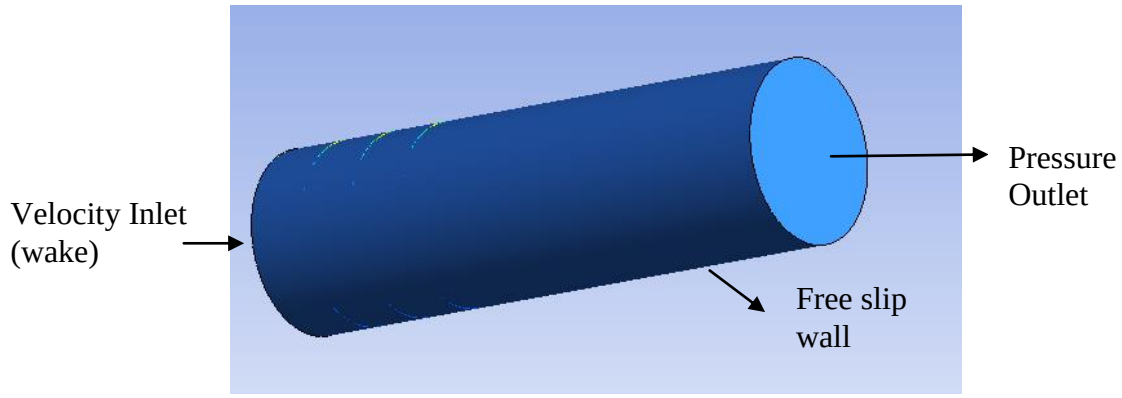

Figure 8. 7: Tunnel used to simulate wake behaviour and boundary condition

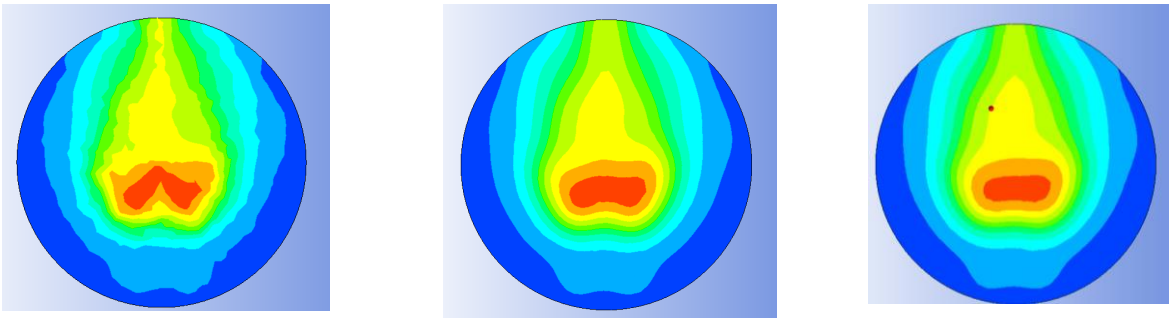

Figure 8. 8: wake at inlet(left) , at 0.5D from inlet(Centre) and 1D from inlet(right)

The introduction tunnel proved to be very effective at preventing dilution of wake. The tunnel also allows sufficient gap between the propeller and the inlet to avoid suction effect. The simulation is performed in both model scale and full scale to allow direct comparison between the methods. The simulation is also performed at J values ranging from 0.15 to 0.65. FEA analysis is then performed to find the structural assessment at all the J values.

8.2.1 Wake applied

The wake applied to the simulation is the effective wake from behind ship condition mentioned in section 6.The model scale wake applied and the full scale wake applied is shown in Figure 6.14. A simulation is carried with nominal wake provided by MMG but it is found to overpredict or underpredict the results (Figure A2 and Table A1).Ideally, wake values are measured at the propeller plane. The wake contours used for these simulations are taken at upstream interface boundary of the propeller and not at the propeller plane (Figure 8.9). This is because wake cannot be assessed at propeller plane due to the presence of propeller blades. These are the effective wakes at behind ship simulation performed at J values of 0.4458. But, the calculated wake fraction of these contours showed a J value corresponding to 0.53 at model scale and full scale. This is because of the suction generated by the propeller upstream. To understand the influence, a plane is cut at similar distance upstream to the propeller of the open water test performed at J value corresponding to 0.45 (Figure 8.10).The wake fraction and corresponding J values are calculated at this location and the comparison is noted in Table 8.3.

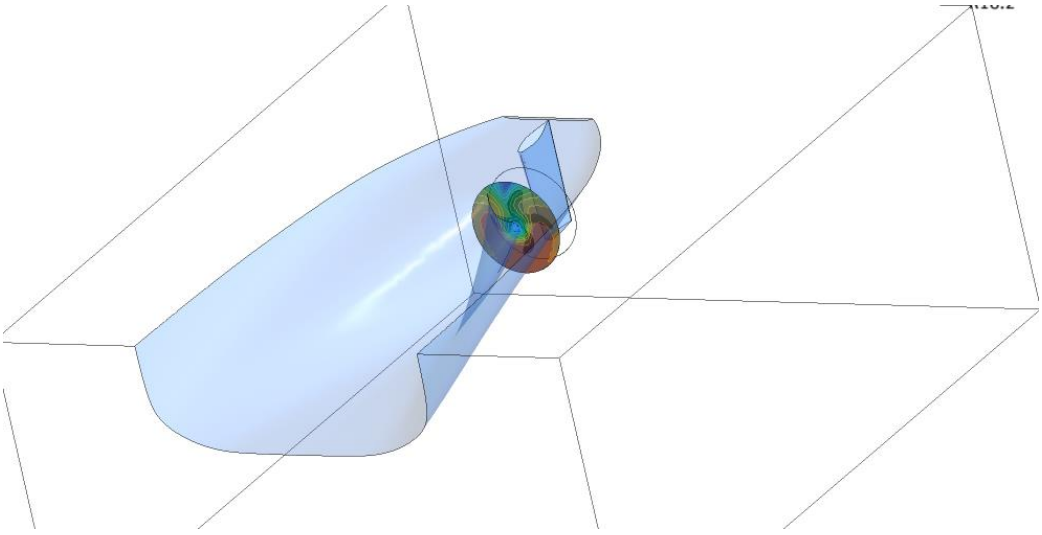

Figure 8. 9: effective wake location behind ship

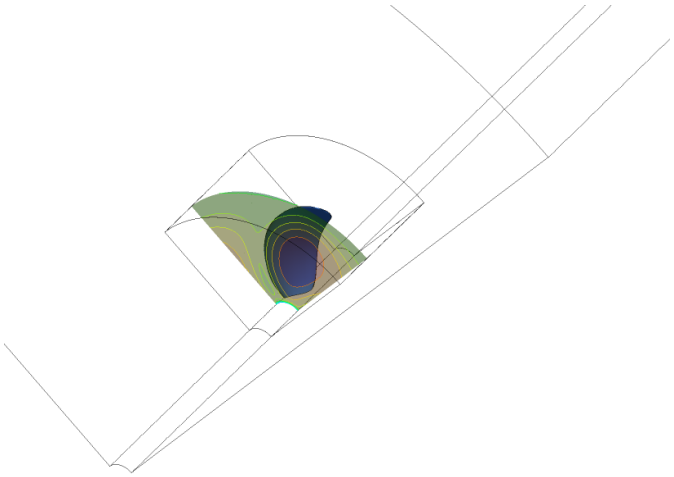

Figure 8. 10: effective wake location open water

Behind ship		Open water	
V_A	0.892	V_A	2.021
n	7.953	n	18
D	0.21	D	0.21
J	0.534	J	0.534

Table 8. 3: comparison of wake characteristics and corresponding J

Both show a similar value of J indicating that the suction effect is consistent in both behind ship and open water condition. Since this wake had to be used as input for the reduced behind ship simulation the J value of the wake is updated to J value of 0.53.Since the reduced behind ship calculation will be performed at RPS of 23.9, the V_A of model scale is updated.To calculate wake contours for J values ranging from 0.15 to 0.65. The wake at J of 0.53 is amplified and reduced to meet the required J values.

8.2.2 Numerical setup

The domain is split into two domain, inner domain and outer domain. Similar to behind ship condition in Section 5, the propeller is studied at transient condition. The inner domain is specified as a rotating domain with RPS kept constant at 23.9 at model scale and 1.452 at Full scale. Figure 8.11 and 8.12 shows the inner and outer domain boundaries and dimensions.

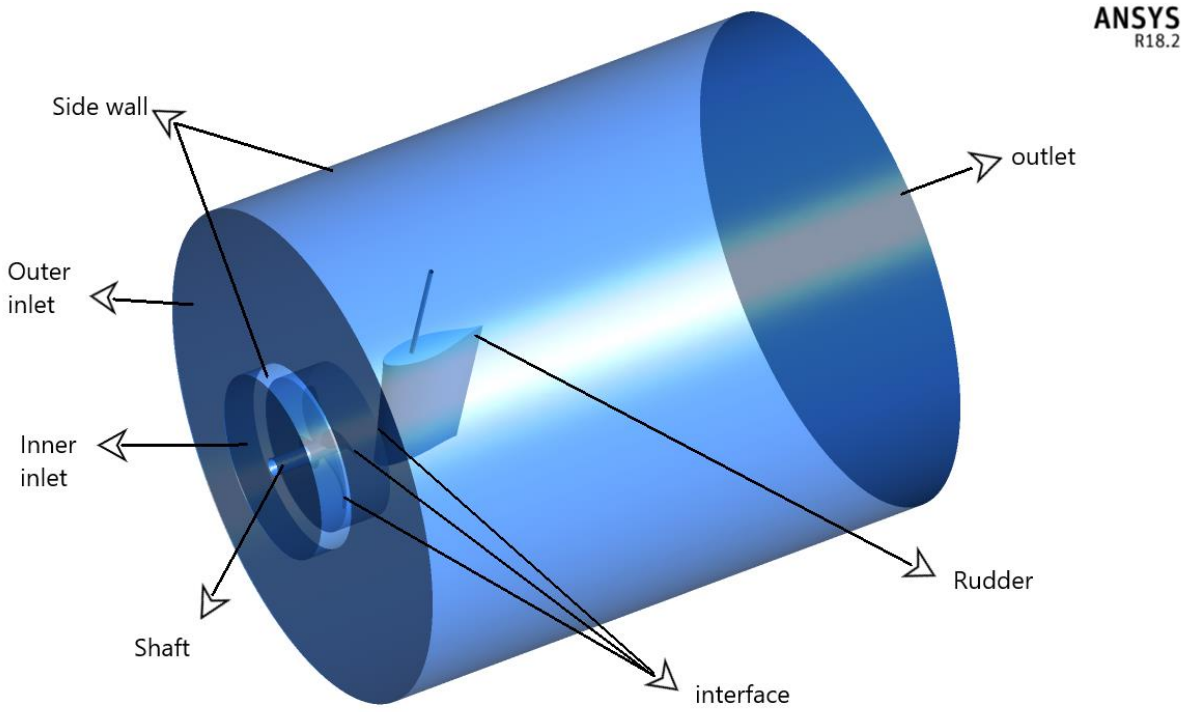

Figure 8. 11: Boundaries of outer domain

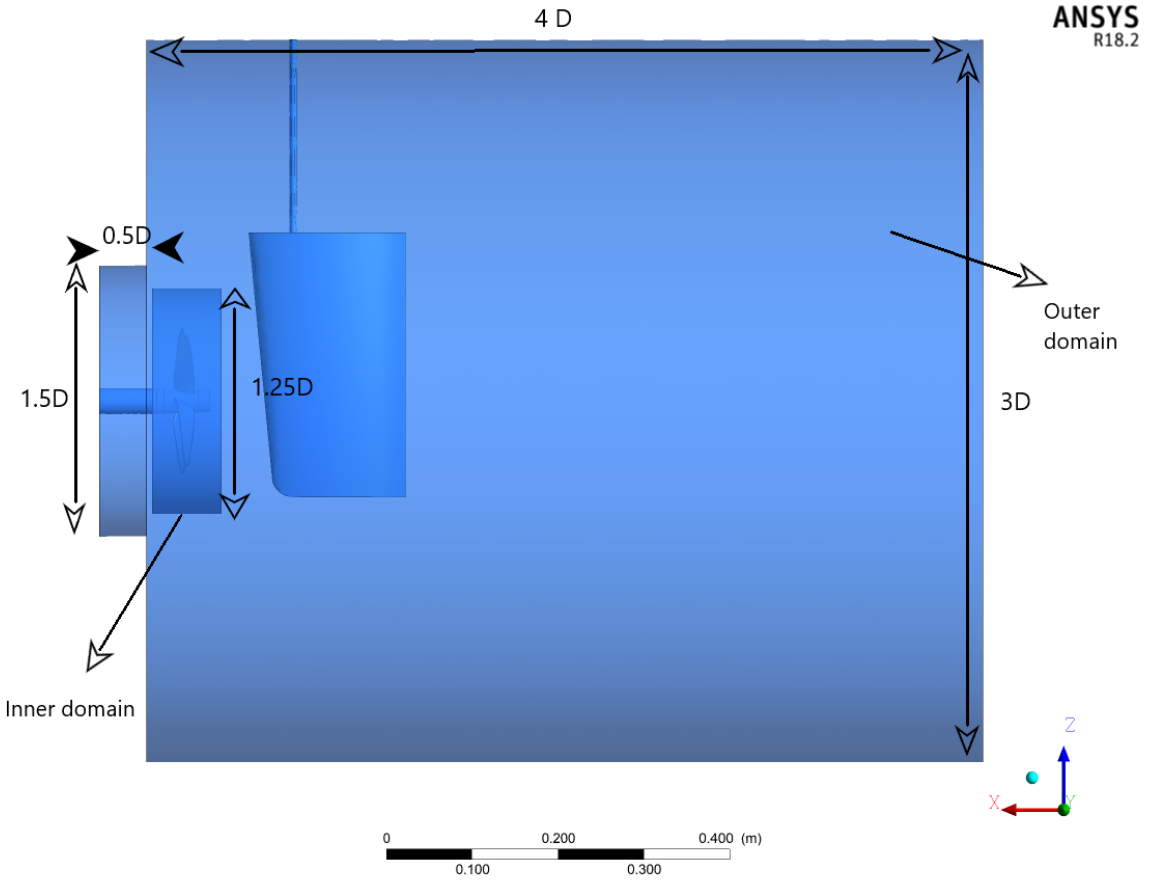

Figure 8. 12: Outer domain dimension

The boundary conditions of outer domain are shown in Table 8.4

Boundary	condition
Inner inlet , Outer inlet	velocity inlet
side wall and shaft	Free slip wall
Rudder	No-slip wall
Outlet	pressure outlet
interface	Transient rotor interface

Table 8. 4: Boundary condition of outer domain

The wake at inner inlet is changed according to the required J. The outer domain is specified as a stationary domain and is used to simulated ship wake and propeller wake in the study.

The inner domain boundaries and dimensions are shown in Figure 8.13 and the boundary conditions applied are shown in Table 8.5. The inner domain is defined as a rotating domain. The RPS is kept constant.

Boundary	condition
Interface	Transient rotor interface
Blades , hub , spacer and cap	No slip wall

Table 8. 5: Boundary conditions of Inner domain

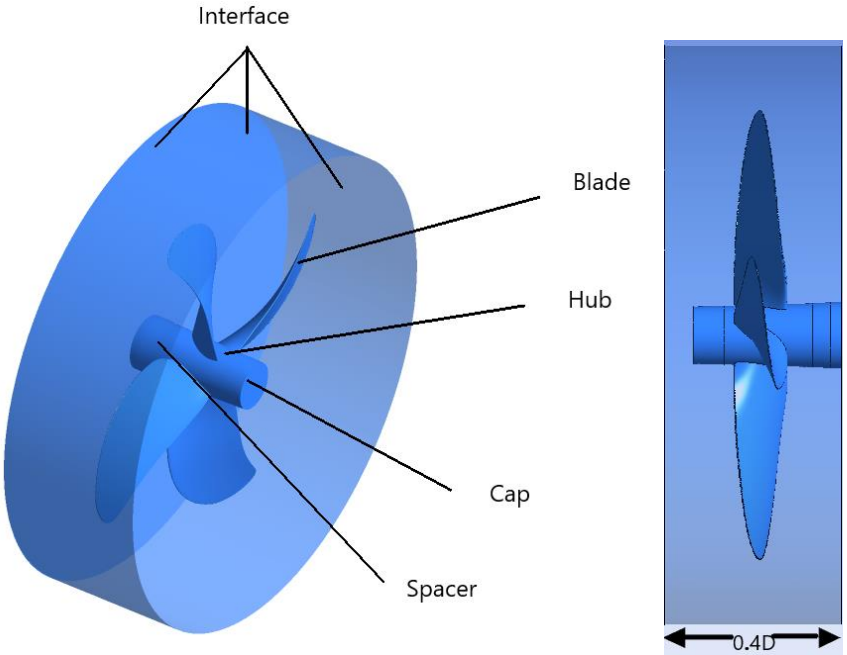

Figure 8. 13: Boundaries of inner domain and dimension

Similar to all other simulations k-ω SST model is used to estimate turbulence. A stepping function same as behind ship condition is applied to reduce time steps as simulation progressed.To reduce computation time and increase convergence rate, the converged solution from previous simulation is used as initial condition for subsequent simulations.

8.2.3 Mesh

The inner and outer domains are meshed separately. The outer domain is meshed without inflation layer and inner domain is meshed with more refinement with the addition of inflation layers to capture boundary layer. Tetrahedral mesh is used to mesh both the domains. Figure 8.14 shows the mesh used for simulation.

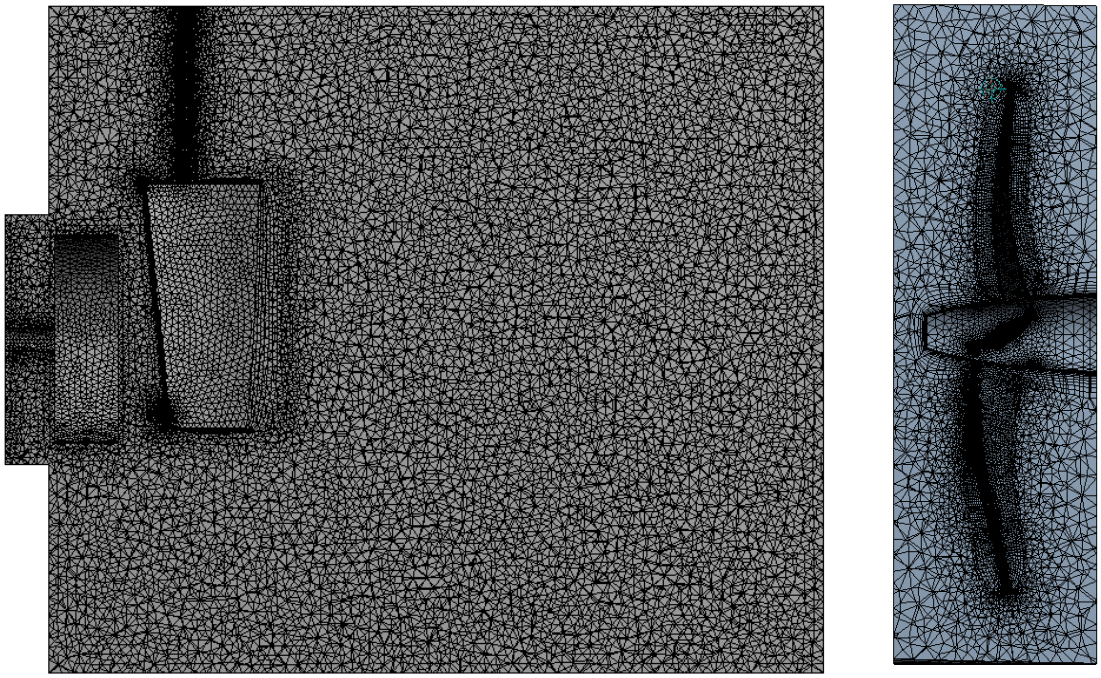

Figure 8. 14: Outer domain mesh (left) and inner domain mesh (right)

A similar mesh configuration to behind ship condition is used and The first layer thickness of the mesh is given a value suitable to ensure that the wall Y+ > 30. A smooth transition between the final inflation layer and the outside cells is ensured by changing number of layers of inflation and growth rate of the inflation layer.

8.2.4 Results and discussion

The results obtained for each J value in reduced behind ship condition are shown in Table 8.6 and Table 8.7

FULL SCALE	Experimental	Numerical	
J	K_T	K_T	Error (%)
0.15	0.3208	0.353	10.17
0.25	0.2849	0.313	9.71
0.35	0.248	0.268	8.11
0.45	0.2096	0.217	3.74
0.55	0.1689	0.164	-2.92
0.65	0.1247	0.106	-15.18

Table 8. 6: Full scale reduced behind ship condition results

MODEL SCALE	Experimental	Numerical	
J	K_T	K_T	Error (%)
0.15	0.3208	0.362	12.860
0.25	0.2849	0.319	11.941
0.35	0.248	0.276	11.164
0.45	0.2096	0.228	8.602
0.55	0.1689	0.177	4.668
0.65	0.1247	0.123	-1.407

Table 8. 7: Model scale reduced behind ship condition results

These results show a similar trend in error. At higher loading (low J) of propeller blade the errors are higher and also over predicted while as the loading reduces the results are eventually under predicted. At J value of 0.55 the error is very low. This is the closest J value to to original wake. This indicates that the domain is very good at predicting behind ship condition but also suffers from accuracy of wake. But at the same time, this domain is a very good option for preliminary analysis with very low computation cost.

The change in flow as the J values changes can be seen in Figures 8.15, 8.16 and 8.17.These Figures are taken at maximum thrust point of blade. At lower J values the suction effect of propeller is very high and also results in suction of water from downstream of the propeller

blades. The flow changes as J increase and eventually results in smooth flow. The drastic flow change at the indicated red region is due slower wake velocities (Figure 6.14) compared to indicated blue region where the flow has much higher velocity.

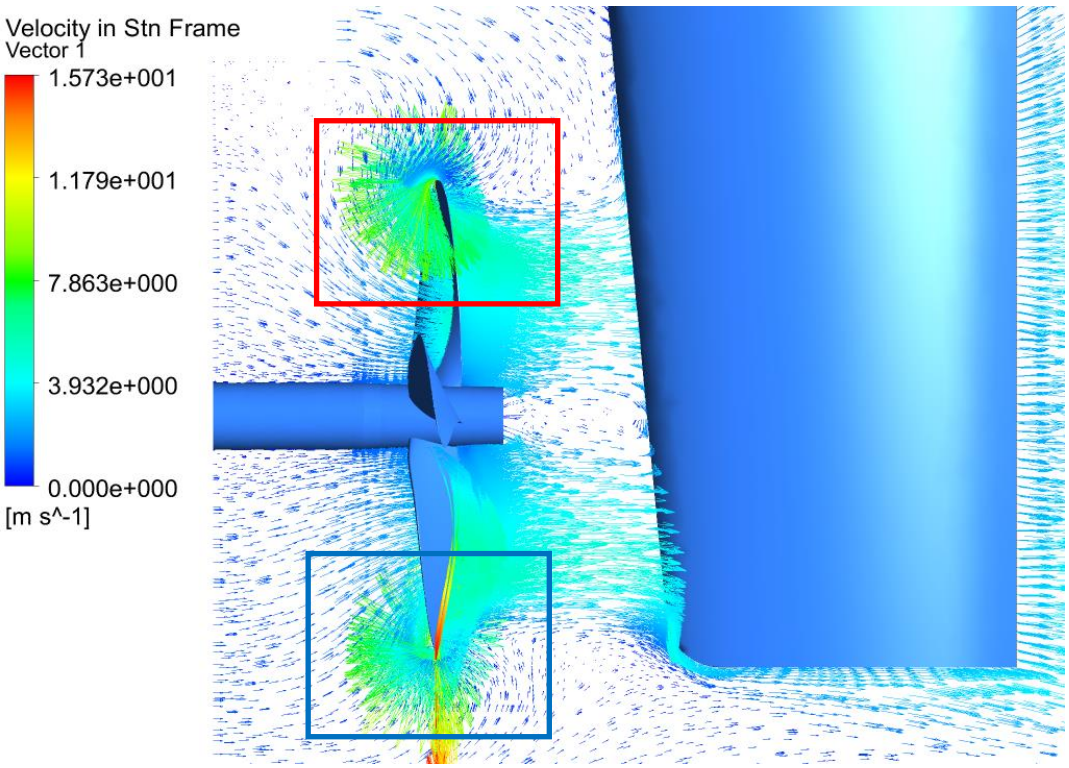

Figure 8. 15: Flow at 0.15 J

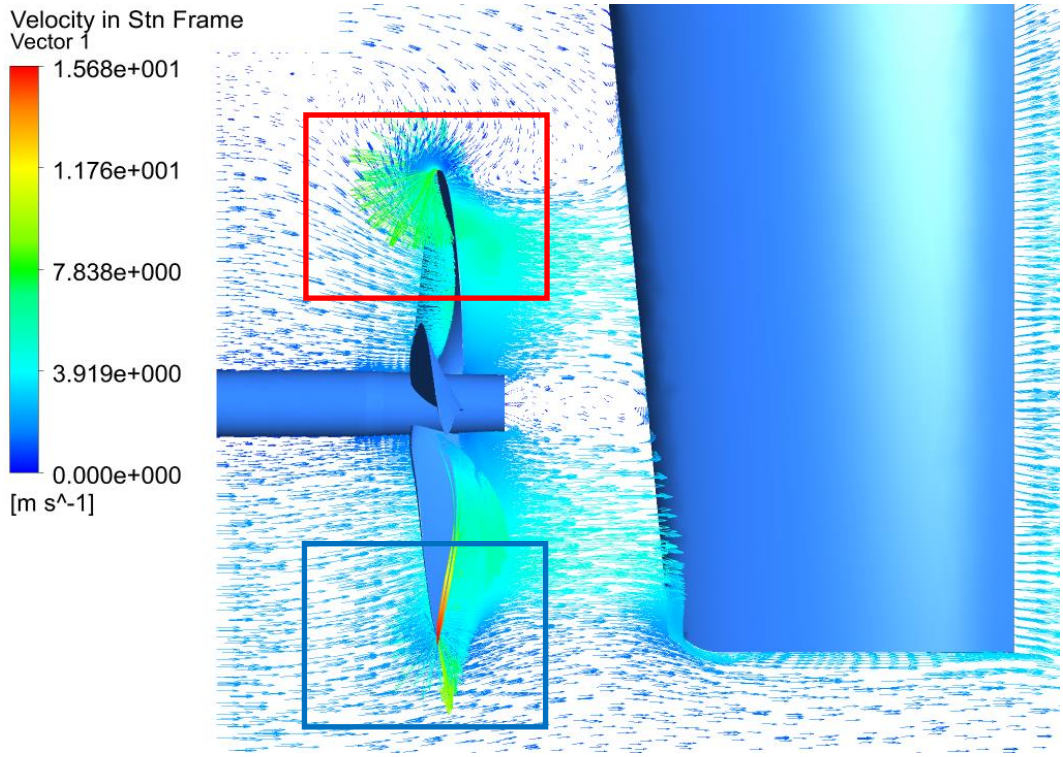

Figure 8. 16: Flow at 0.35 J

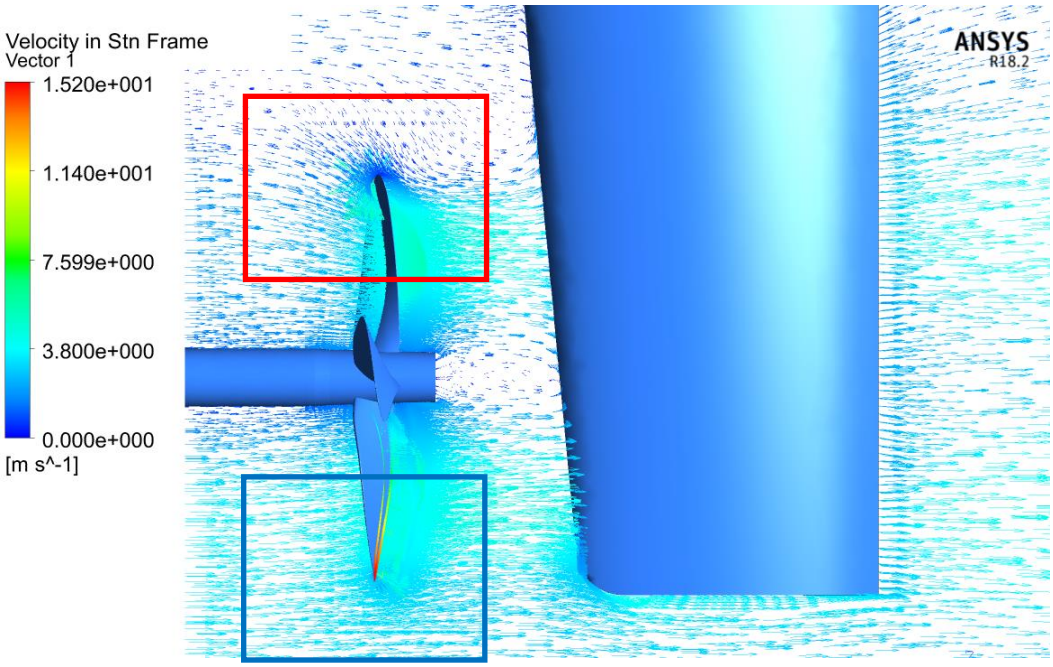

Figure 8. 17: Flow at 0.55 J

8.2.4.1 Wake and focus points

The difference in wake profile (Figure 6.14) has a profound effect on the rotation point at which the focus points are concentrated. The analysis from J values of 0.15 to 0.65 shows a difference in region where the focus points are concentrated. This is shown in Figure 8.18.

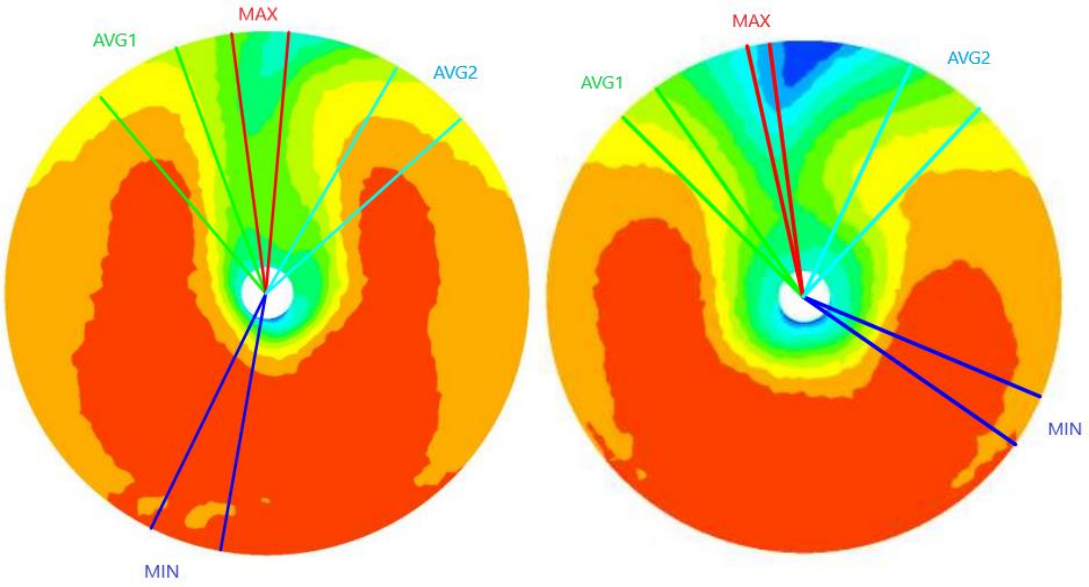

Figure 8. 18: Focus points in Full scale (left) and Model scale (right)

At these focus points it can also be noted that the velocity profile at each radius is also different. This results in centre of pressure shifting along the radius of the blade.

8.3 FEA analysis of reduced behind ship condition

The structural assessment of the blade is performed at each J value ranging from 0.15 to 0.65. The procedure, numerical setup and boundary conditions for the FEA analysis are identical to the FEA analysis performed in Section 6. In this section, the results of full scale analysis are considered as the benchmark and the difference in the scaling effects of model scale and its effects are discussed. Similar to the results in Section 6, the focus of this section will also be on the structral analysis at maximum thrust focus point. Therefore in this section, a detailed analysis shows stress, strain and deformation developed and the reason for this error.

All results shown below are comparison of Maximum thrust point results. Figure 8.19 shows the error in stress, strain and deformation at each J value. Figure 8.20 shows the error in centre of pressure, reaction forces and reaction moment generated at associated J values. The overall trend can be broken down to two sections. A contribution of reaction force and a contribution by centre of pressure. The reaction force clearly dictates whether the stress is overpredicted or under predicted at each J value. While the location of centre of pressure dictates the magnitude of error. A positive error of centre of pressure indicates that the scaled model scale CFD pressure has a centre of pressure at a longer distance (towards the tip) than full scale centre of pressure.J value of 0.35 can be considered as break even point where the centre of pressure flips to over prediction compared to full scale. From this point forward, the stresses developed are over prediction.

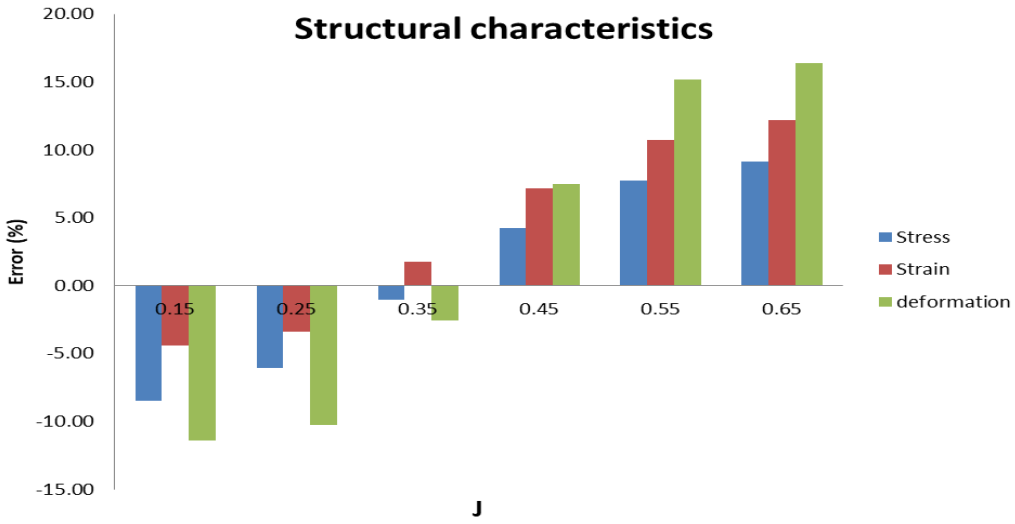

Figure 8. 19: Structural error across different J values

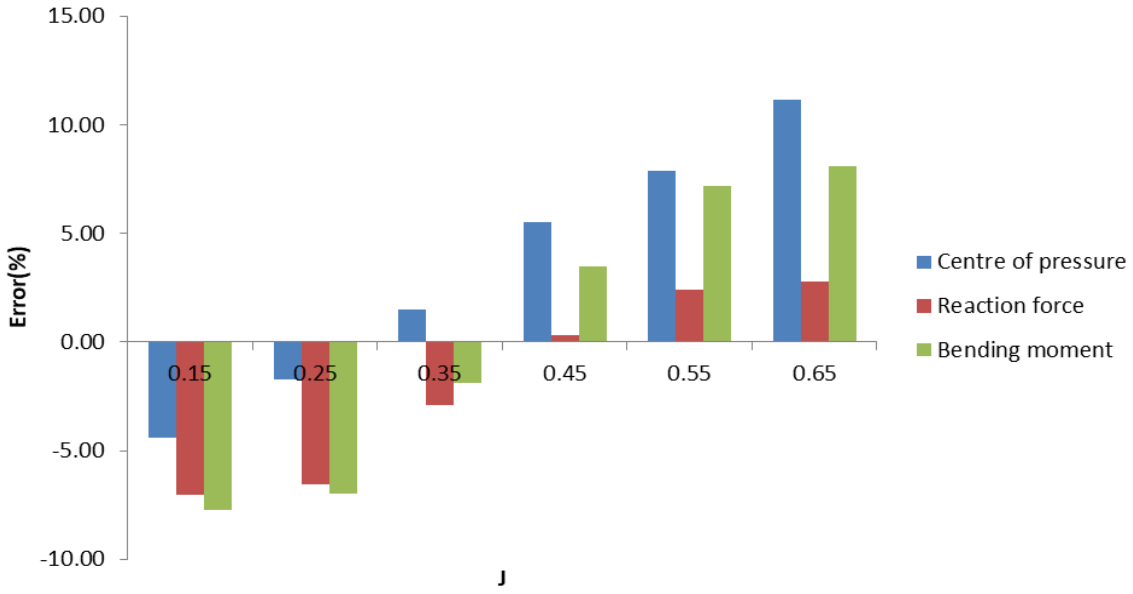

Figure 8. 20: Error chart of centre of pressure, reaction force and reaction moment

The contribution of centre of pressure can be observed clearly at J value of 0.65. The high positive error of centre of pressure at J of 0.65 drives the bending moment error. This increases the bending stress, which increases the overall von mises stress. The deformation is also severely effected as the centre of pressure is more towards the tip of the blade , which contributes to higher deformation.

Figures 8.19 also shows that at very low J values the method underpredicts the stress and at higher J values it over predicts the stress. This is again depended on the centre of pressure which is inturn dependent on the wake applied. But, at the same time the errors are less than 20% at the extremes, which means the method could be used as a first estimate for structural characteristics. The contribution of both wake and Cp are present in this results and yet the overall predictions proves to be quiet good especially considering the reduction in computational cost.

9. CONCLUSION

The implemented fluid-structure coupling shows promising results. Two levels of reduction from usual domain for behind ship conditions are discussed in this thesis. The domain discussed in section 6 offers better and accurate results with reduction in computational cost, although achieving convergence takes longer time. But still better compared with usual “full size” domain where entire ships are modelled.

The scaling of pressure points using Cp, to achieve coupling shows good results. This helps prevent costly computations at full scale. It should be noted that laminar flow could be present in model scale which is absent in full scale especially at low inflow speeds and propeller rpm. Therefore, scaling these results could result in gross over prediction.

The reduced domain shows good results, but is dependent on the wake given as inlet. But, assuming the wake at inlet is accurate; the method shows very fast convergence and accurate results. If proper wake is not applied, gross over prediction or under prediction of structural analysis can be expected as the stresses developed on the blade are highly dependent on the centre of pressure. Therefore, the reduced method coupling is only recommended if good wake values are available. Nominal wake can be used for this simulation but tunnel has to be much longer to allow suction to occur but then the influence of longer tunnel on flow should be investigated. Effective wake, if known is the best option, but requires higher computational cost to predict. The former method is suggested if no wake data’s are available.

Overall, this thesis shows that fluid structure interactions need not be as computationally intensive as expected. Reasonable assumptions and proper implementation to achieve what is actually required could cut down resource requirements and time. Both levels of reduction suggested in the thesis yields very good results.

10. ACKOWLEDGEMENT

This thesis is possible only because of the enormous support and assistance provided by all staff at MMG. There are numerous people I would like to thank for their help and to begin with, I would like to thank my supervisor at MMG, Mr Lutz Kleinsorge for his invaluable presence, support and guidance. This thesis would not have even been half as good without his contribution. I would also like to thank Mr Tom Goedicke and Mr Robert Tietze of MMG for their insights and guidance.

I would like to thank Prof.Lionel Gentaz, my supervisor from Ecole Centrale Nantes, France and also all my professors at ECN for educating me to the point where I can think and work on my own.

I am also grateful to all the MMG staff who always had a smile on their face and welcomed me into their company. It has been a pleasure to work with you all.

Also, I would like to thank all my batch mates and friends, who always supported me and made me laugh.

I sincerely thank the people behind Erasmus program and EMShip for helping me achieve this goal and allowing me to come here and achieve high level of education. Your contribution will remain invaluable.

11. REFERENCES

1. ANSYS documentation version 18.2, referencing guide, CFX manual, chapter 5.2.1 unidirectional (One-way) FSI
2. Bertram, Volker. , 2012a *Practical ship hydrodynamics*. Elsevier
3. Germanischer Lloyd, 2017 ,Rules for Classification and Construction Ship Technology, Chapter 6
4. Ghose and Ghokarn , 2004a. *Basic Ship Propulsion*. Allied Publishers New Delhi
5. ITTC. (2008) 'ITTC – Recommended Procedures and Guidelines: Performance, Propulsion 1978 ITTC Performance Prediction Method'. 25th ITTC
6. John Carlton, 2007. *Marine Propellers and Propulsion* Butterworth-Heinemann Great Britain
7. Mert Gokdepe, 2015, *Turbulence Models for the Numerical Prediction of Transitional Flows with RANSE*, thesis (Master), Massachusetts Institute of Technology
8. MIT hydrodynamics handout, http://web.mit.edu/2.016/www/handouts/2005Reading10.pdf
9. Shin, Keun Woo and Andersen, Poul , 2017 *CFD Analysis of Scale Effects on Conventional and Tip-Modified Propellers* , Fifth International Symposium on Marine Propulsors - smp'17
10. SVA open water test ,https://www.sva-potsdam.de/en/open-water-test/

12. APPENDIX

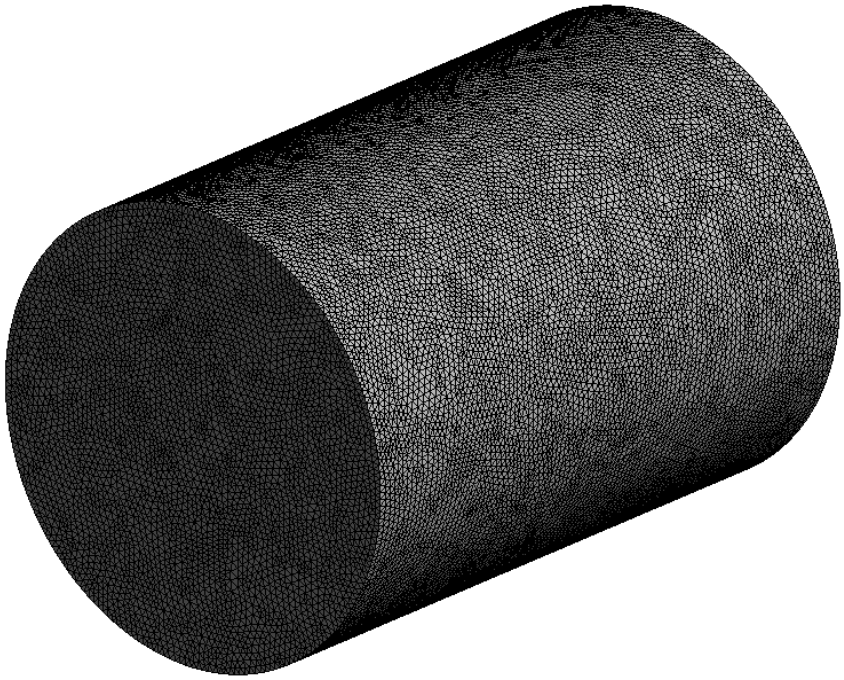

Figure A1:Domain mesh

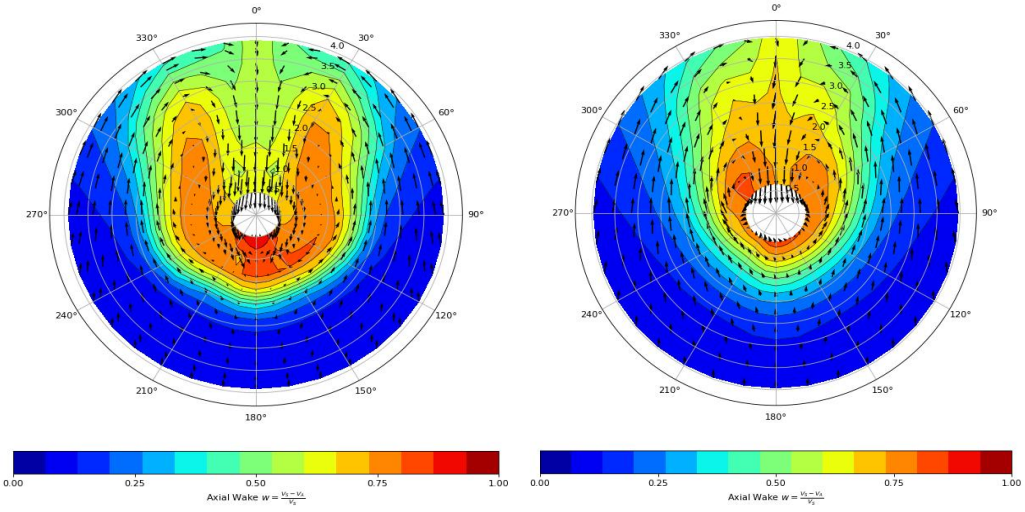

Figure A2 : MMG provided wake from OFpimple (left) and Fine Marine (right)

wake	Study type	J = 0.4458			
		Thrust (N)	Torque (N.m)	KT	10KQ
	experimental	23.13	0.597	0.188	0.231
Without rudder					
OFpimple	Simulation	26.500	0.713	0.216	0.277
	Error (%)	14.57	19.46	14.78	19.68
with rudder					
OFpimple	Simulation	26.920	0.717	0.220	0.278
	Error (%)	16.39	20.08	16.60	20.30
Finer Marine	Simulation	16.125	0.513	0.131	0.199
	Error (%)	30.29	14.15	30.16	14.00

Table A1: Results of reduced domain analysis using different nominal wakes